Vimentin organization modulates the formation of lamellipodia

Brian T. Helfand[a,*], Melissa G. Mendez[b,*], S. N. Prasanna Murthy[b], Dale K. Shumaker[a], Boris Grin[b], Saleemulla Mahammad[b], Ueli Aebi[c], Tatjana Wedig[d], Yi I. Wu[e], Klaus M. Hahn[f], Masaki Inagaki[g], Harald Herrmann[d], and Robert D. Goldman[b]

Departments of [a]Urology and [b]Cell and Molecular Biology, Feinberg School of Medicine, Northwestern University, Chicago, IL 60611; [c]M.E. Müller Institute for Structural Biology, Biozentrum, University of Basel, CH-4056 Basel, Switzerland; [d]Department Molecular Genetics, German Cancer Research Center (DKFZ), 69120 Heidelberg, Germany; [e]University of Connecticut Health Center, Farmington, CT 06030; [f]Department of Pharmacology, University of North Carolina School of Medicine, Chapel Hill, NC 27599; [g]Division of Biochemistry, Aichi Cancer Center Research Institute, Chikusa-ku, Nagoya, Aichi 464-8681, Japan

ABSTRACT **Vimentin intermediate filaments (VIF) extend throughout the rear and perinuclear regions of migrating fibroblasts, but only nonfilamentous vimentin particles are present in lamellipodial regions. In contrast, VIF networks extend to the entire cell periphery in serum-starved or nonmotile fibroblasts. Upon serum addition or activation of Rac1, VIF are rapidly phosphorylated at Ser-38, a p21-activated kinase phosphorylation site. This phosphorylation of vimentin is coincident with VIF disassembly at and retraction from the cell surface where lamellipodia form. Furthermore, local induction of photoactivatable Rac1 or the microinjection of a vimentin mimetic peptide (2B2) disassemble VIF at sites where lamellipodia subsequently form. When vimentin organization is disrupted by a dominant-negative mutant or by silencing, there is a loss of polarity, as evidenced by the formation of lamellipodia encircling the entire cell, as well as reduced cell motility. These findings demonstrate an antagonistic relationship between VIF and the formation of lamellipodia.**

Monitoring Editor
M. Bishr Omary
University of Michigan

Received: Aug 17, 2010
Revised: Jan 4, 2011
Accepted: Feb 10, 2011

INTRODUCTION

Cell migration is an essential feature of many normal and pathological processes including embryogenesis, wound healing, inflammatory responses, and tumor cell metastasis. During migration, cells form dynamic or ruffled membranes that define the leading edges of motile cells. The formation of lamellipodia is thought to be regulated almost entirely by the assembly of an intricate network of filamentous (F)-actin and actin-associated proteins. It is well established that actin filaments, the Arp 2/3 complex and N-WASP, regulated by various small Rho-family GTPases (e.g., Rac1, RhoA, and Cdc42) and actin capping/binding proteins (cofilin and profilin) are universal components of lamellipodia (Small *et al.*, 2002; Takenawa and Suetsugu, 2007). Additionally, microtubules and other cytoskeletal-binding proteins such as fascin, fimbrin, dynamin, and cortactin influence actin network behavior and thereby contribute to the formation of lamellipodia (Matsudaira, 1994; Mogilner and Keren, 2009; Yamada *et al.*, 2009). Numerous kinases involved in different signal transduction pathways (e.g., extracellular signal–regulated kinase, c-Jun N-terminal kinase, p21-activated kinase [PAK], and protein kinase A) are also involved in initiating the formation of lamellipodia (Hall, 2005). The coordination and integration of all of these factors is essential for the control of actin polymerization within lamellipodia, which in turn is required for cell motility.

Vimentin, a type III intermediate filament (IF) protein, is a major cytoskeletal component of motile mesenchymal cells, including fibroblasts, macrophages, and metastatic tumor cells of epithelial origin. Vimentin, like other cytoskeletal IF, forms a complex network

This article was published online ahead of print in MBoC in Press (http://www.molbiolcell.org/cgi/doi/10.1091/mbc.E10-08-0699) on February 23, 2011.

*These authors contributed equally to this work.

Address correspondence to: Robert D. Goldman (r-goldman@northwestern.edu).

Abbreviations used: BSA, bovine serum albumin; EMT, epithelial-to-mesenchymal transition; FCS, fetal calf serum; FRAP, fluorescence recovery after photobleaching; GFP, green fluorescent protein; IF, intermediate filament; mEF, mouse embryo fibroblast; NA, numerical aperture; PA, photoactivatable; PAK, p21-activated kinase; PBS, phosphate-buffered saline; pEGFP, plasmid enhanced green fluorescent protein; PI3Kγ, phosphoinositide 3-kinase γ; PKC, protein kinase C; shRNA, short-hairpin RNA; ULF, unit-length filament; VASP, vasodilator-stimulated phosphoprotein; VIF, vimentin intermediate filament.

that circumscribes the nucleus and radiates toward the cell periphery. There is evidence that these vimentin IF (VIF) are involved in the regulation of cell motility. For example, vimentin expression has been correlated with cell migration in wound healing in normal cultured epithelial cells (Gilles *et al.*, 1999). It has also been shown that vimentin-knockout mice are defective in wound healing, that fibroblasts from the embryos of these mice are incapable of translocation, and that the reintroduction of vimentin rescues the motility of these cells (Eckes *et al.*, 1998, 2000; Mendez *et al.*, 2010). Other evidence supporting the role of vimentin in cell motility comes from studies of the epithelial-to-mesenchymal transition (EMT; Acloque *et al.*, 2009). Intriguingly, vimentin expression alters the shape and enhances the motility of epithelial cells during the EMT, which takes place in normal development and tumor cell metastasis (Hendrix *et al.*, 1997; Mendez *et al.*, 2010). Similarly, analysis of the IF content of cancer cells demonstrates that vimentin expression is highly correlated with the invasive potential of many epithelial-derived cancers including those of the prostate and breast (Vora *et al.*, 2009; Zhang *et al.*, 2009), whereas the silencing of vimentin expression decreases the invasive properties of breast carcinoma cells by inhibiting the elongation of invadopodia (Schoumacher *et al.*, 2010).

In spite of the evidence supporting a role for VIF in cell motility, their specific function(s) have yet to be defined. It is likely that their organization and assembly states are altered as cells change shape during cell movement. With regard to the assembly states of VIF, it has been shown in vitro that vimentin assembly occurs in a stepwise hierarchical manner from soluble tetrameric complexes to mature IF (Herrmann and Aebi, 2000). An important intermediate in the assembly process is the unit-length filament (ULF) that is generated by the lateral association of eight tetramers. Notably, a vimentin mutant, Y117L, which exclusively forms ULF in vitro under a variety of buffer conditions, assembles into minuscule rodlets only when synthesized in vivo by forced expression in vimentin-free fibroblasts (Meier *et al.*, 2009). This suggests that ULF are formed in living cells. Nonfilamentous vimentin particles, which may represent aggregates of ULF, appear to be precursors in the assembly of short IF (squiggles), which then join end to end to form the long, mature IF that characterize the extensive networks present throughout interphase cells (Prahlad *et al.*, 1998; Kirmse *et al.*, 2007). Mature IF are dynamic structures as evidenced by fluorescence recovery after photobleaching (FRAP) analyses showing their constant exchange of subunits (Yoon *et al.*, 1998) and their continuous bending and waveform movements (Ho *et al.*, 1998; Yoon *et al.*, 1998).

With respect to the regulation of these assembly states of VIF in vivo, it has been shown that phosphorylation influences the dynamic properties of IF subunit exchange and VIF organization in cells (e.g., Chou *et al.*, 1990; Sihag *et al.*, 2007; Hyder *et al.*, 2008). Human vimentin has >40 known phosphorylation sites (Li *et al.*, 2002), many of which are targets of kinases involved in regulating cell motility and related processes (Sihag *et al.*, 2007). For example, the phosphorylation of vimentin by phosphoinositide 3-kinase γ (PI3Kγ), which is involved in chemotaxis and cell migration, induces VIF network retraction toward the nucleus, while the expression of a PI3Kγ-insensitive vimentin mutant shows no retraction (Barberis *et al.*, 2009). In addition, immunofluorescence observations suggest that VIF organization is regulated by RhoA-binding kinase, ROKα, which is known to promote the formation of stress fibers and focal adhesion complexes (Sin *et al.*, 1998). The organization and phosphorylation of vimentin is also affected by many other kinases with known roles in cell motility (Sihag *et al.*, 2007).

In this study, we have experimentally interfered with VIF assembly and organization in order to gain insights into their functions in cell motility. Our results show that VIF at the periphery of fibroblasts inhibit the formation of lamellipodia, whereas the disassembly and withdrawal of VIF from the cell periphery facilitate the actin-based protrusion of lamellipodia.

RESULTS

Vimentin organization within moving fibroblasts: lamella and lamellipodia

To initiate these studies, we determined the distribution of the different assembly states of vimentin in 3T3 cells and mouse embryo fibroblasts (mEF), both of which exhibit the typical fan-shaped leading lamellipodium and lamella of motile cells (Figure 1A). Complex networks of long VIF are concentrated in the tail and perinuclear regions of these cells, with fewer long VIF extending from the nuclear region into the lamella (Figure 1B). The majority of these long VIF terminate in the proximal region of the lamella, where there is an increase in the number of short filaments (squiggles; Figure 1C, see region a) and nonfilamentous vimentin precursor particles (Figure 1C, see region b). The number of squiggles decreases in the more distal regions of the lamella, while the number of particles increases. Within leading lamellipodia, there is a significant enrichment of particles (Figure 1C, see region c). Overall, we observe an apparent gradient of the assembly forms of vimentin such that the highest concentration of vimentin particles is in lamellipodia, while the highest concentrations of long VIF are in the tail and perinuclear regions (Figure 1, B and C). Observations of live fibroblasts expressing green fluorescent protein (GFP)–vimentin show virtually identical distributions of these different forms of vimentin, although there appear to be fewer particles in lamellipodia due to rapid photobleaching (Figure 2, A–C). To localize the different assembly forms of vimentin within lamella and lamellipodia more precisely, we used antibodies directed against well-established lamellipodial markers including actin, Arp2/3, vasodilator-stimulated phosphoprotein (VASP), and cortactin (Small and Resch, 2005). Double-label immunofluorescence revealed the presence of nonfilamentous vimentin particles in the same regions as these markers (Supplemental Figure S1, A–I). Platinum replica immunogold electron microscope preparations confirmed the presence of vimentin particles in close association with the actin network within lamellipodia (Supplemental Figure S1, J–L).

Vimentin disassembly and retraction accompanies the induction of lamellipodia in serum-starved cells

When fibroblasts are deprived of serum for 24–72 h, the frequency of lamellipodia formation decreases and the majority of cells adopt more rigid-appearing cellular margins (Figure 1D). More specifically, 65% (n = 100) and 80% (n = 100) of serum-free 3T3 fibroblasts had no lamellipodia after 48 and 72 h, respectively, as indicated by Arp2/3 staining (data not shown). In contrast, in medium containing serum, the majority of cells (90%; n = 100) exhibit ruffled membranes/lamellipodia. After 72 h without serum, the VIF network consisted primarily of long fibrils appearing to extend from the perinuclear region to the cell periphery (Figure 1, E and F), with only a few particles and short filaments visible in the cytoplasm. Within 1 min following serum addition, long VIF began to retract and lose their close associations with regions of the cell surface where membrane ruffling was initiated. Coincident with this rapid reorganization of VIF, numerous vimentin particles appeared within seconds, squiggles appeared within minutes, and both of these structures were dispersed in the forming of lamella and lamellipodia. By 30 min after serum addition, the distribution of the different forms of vimentin within cells containing a leading lamellipodium

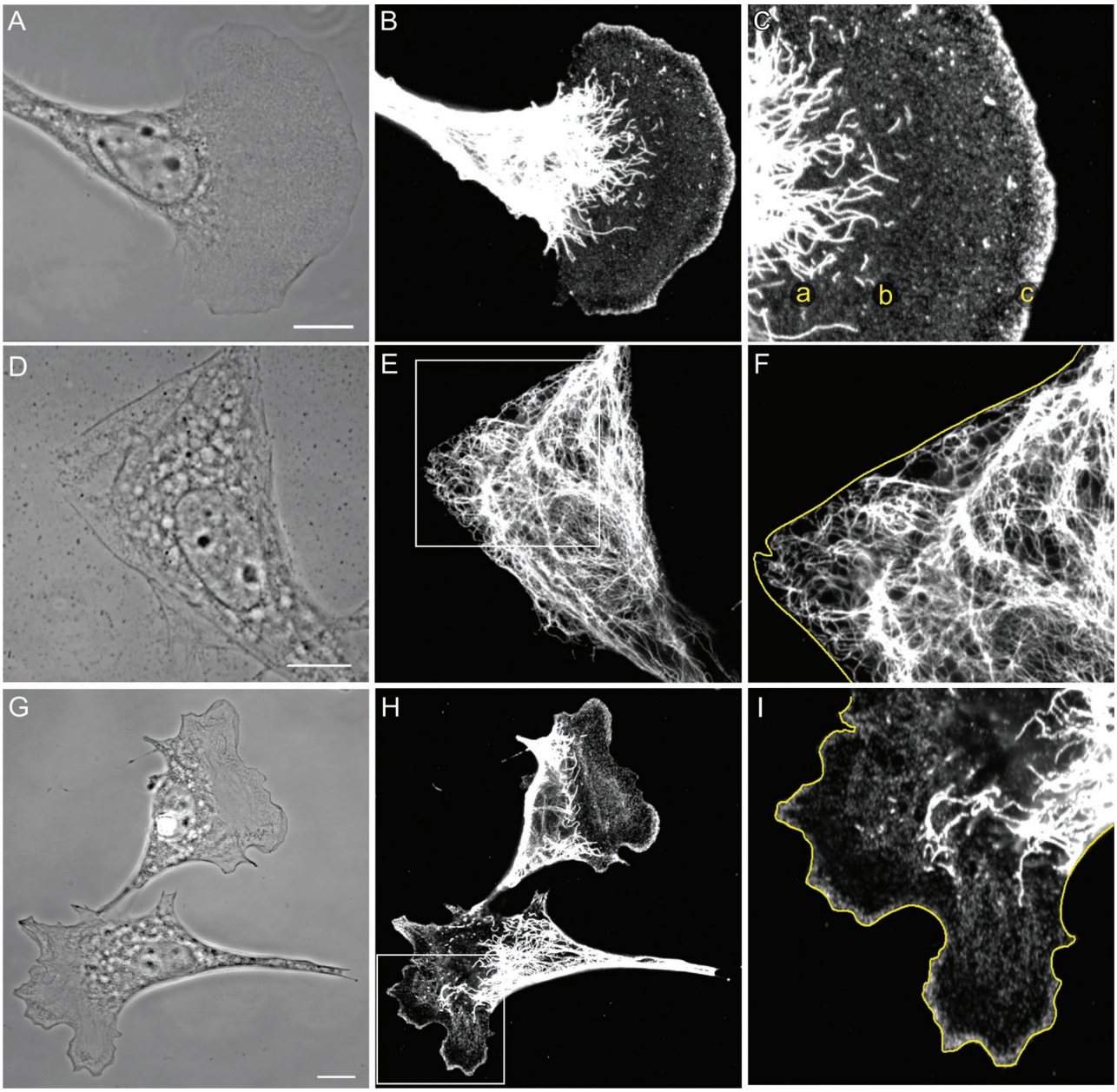

FIGURE 1: (A–C) Vimentin in a motile 3T3 cell with a typical leading lamellipodium and a trailing tail region. Long VIF are abundant in the tail, in the perinuclear regions, and appear to terminate in the proximal regions of the lamella (C, a). Short filaments (squiggles) are present in the proximal portion of the lamella (C, b), and particles are evident throughout the lamella. The lamellipodium is enriched in vimentin particles (C, c; A, phase contrast; B, C, immunofluorescence using anti-vimentin. C is a higher magnification of B). (D–F) Serum-starved 3T3 cells have mainly rigid-appearing edges devoid of lamellipodia (D). VIF extend to the edge of the cell (D, phase contrast; E, immunofluorescence with anti-vimentin; F is a higher magnification of the region in the box in E; cell edge traced in yellow). (G–I) Within minutes of the addition of serum to serum-starved 3T3 cells, areas of membrane ruffling/lamellipodia become apparent (G). After 30 min, immunofluorescence reveals that the distribution of the different forms of vimentin in the lamella/lamellipodia and tail regions are indistinguishable from those seen in fibroblasts maintained in serum (G, phase contrast; H, anti-vimentin; I, higher magnification of boxed area in H; cell edge traced in yellow). Bars = 10 μm.

was indistinguishable from that of cells maintained in normal growth medium (Figure 1, G–I). Observations of the reorganization of Emerald-vimentin expressed in living fibroblasts following serum addition supported these findings, as within minutes the long VIF were retracted from the cell surface toward the nuclear region (Figure 2, D–I). In regions where VIF remained associated with the cell surface, no membrane ruffling was observed. Because the intracellular movements of VIF are known to be regulated to a great extent by motors associated with microtubules and microfilaments, we also examined the retraction of VIF in response to serum in the presence of inhibitors of both of these cytoskeletal systems. Nocodazole was used to disrupt microtubules in serum-starved cells before serum addition (see *Materials and Methods*). Following serum addition, the VIF network exhibited global retraction to the perinuclear region, as ruffling was initiated over the entire cell surface. This demonstrates that microtubules are not required for the

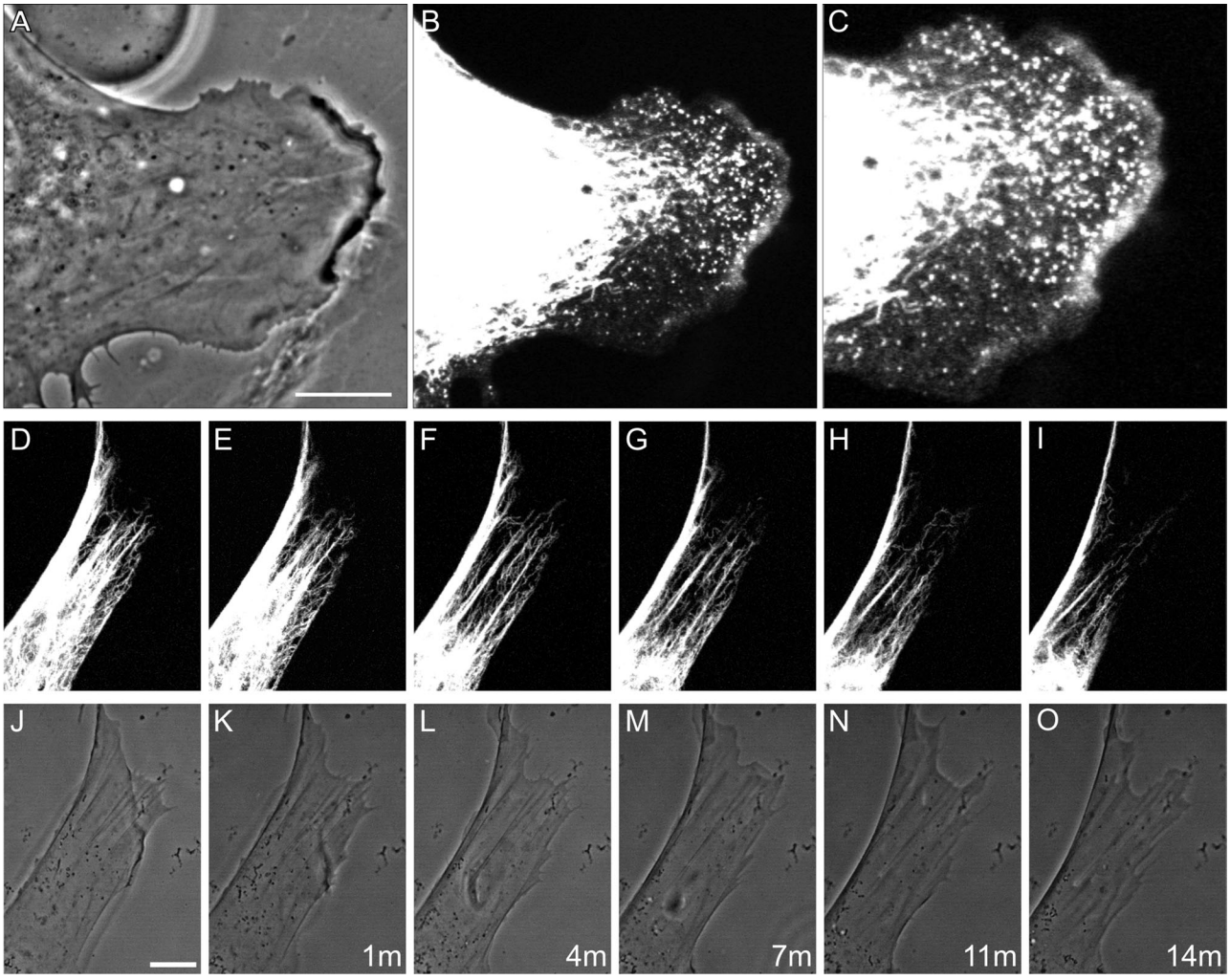

FIGURE 2: Vimentin organization within live and serum-starved cells. (A–C) Observations of a lamellipodium in a live mEF expressing Emerald-vimentin show that long VIF do not extend into lamella/lamellipodia. Note the presence of particles in the lamellipodium with some squiggles in the proximal regions of the lamella. The fluorescence of particles present within the lamellipodium is light-sensitive and fades rapidly (A, phase contrast; B, Emerald-vimentin; C, higher magnification of B). (D–O) Time-lapse series of a region at the edge of a mEF expressing Emerald-vimentin that has been serum starved for 72 h. Top row shows Emerald-vimentin before (D), and at time intervals indicated (E–I), following the addition of serum. VIF retract toward the perinuclear region as membrane ruffles form and squiggles and some particles become visible (J–O, same images in phase contrast). Times indicated are in minutes. Bars = 10 μm.

retrograde movement of VIF (data not shown; Goldman *et al.*, 1996). In the presence of the actin-inhibitors latrunculin A or cytochalasin B, VIF were retained at the cell surface, and membrane ruffling was not evident following serum addition (Hollenbeck *et al.*, 1989).

The dynamic properties and phosphorylation of VIF are altered during the formation of lamellipodia

Subunit exchange along VIF in cells expressing GFP-vimentin was measured by FRAP in serum-starved fibroblasts and following serum addition. Fluorescence recovery was significantly slower in serum-deprived cells ($t_{½}$ = 12.1 ± 2.4 min, n = 10) compared with cells observed 5–10 min following serum addition ($t_{½}$ = 5.7 ± 1.9 min, n = 10; $p < 0.001$). A likely factor involved in the increased rate of subunit exchange is vimentin phosphorylation, which regulates the assembly states, organization, and dynamic properties of IF proteins (Sihag *et al.*, 2007; Hyder *et al.*, 2008). Kinases activated following serum addition include Rho-kinase, protein kinase C (PKC), AKT, and PAK, all of which phosphorylate vimentin Ser-38 (Ando *et al.*, 1989; Kosako *et al.*, 1997; Goto *et al.*, 2002; Eriksson *et al.*, 2004; Zhu *et al.*, 2011). Quantitative immunoblotting confirmed that Ser-38 was rapidly phosphorylated following serum addition, increasing by ~350% in the first minute. This level of phosphorylation persisted for 60 min (Figure 3A) and was comparable to that of cells grown in normal serum (data not shown). To determine whether this rapid increase in Ser-38 phosphorylation was reversible, 72-h serum-starved cells were exposed to a 30-min pulse of serum and then returned to serum-free medium. By 30 min following serum withdrawal, levels of pSer-38 vimentin were significantly decreased, and by 120 min vimentin–Ser-38 phosphorylation resembled that of 72-h serum-starved cells (Figure 3B). Immunofluorescence observations of cells following serum addition confirmed these results (Figure 3, D–L) and demonstrate that VIF, as well as vimentin squiggles and particles (Figure 3, J–L), are phosphorylated at Ser-38 within <1 min following serum addition. Another phosphoepitope-specific antibody, vimentin pSer-82 (Izawa and Inagaki, 2006), showed no

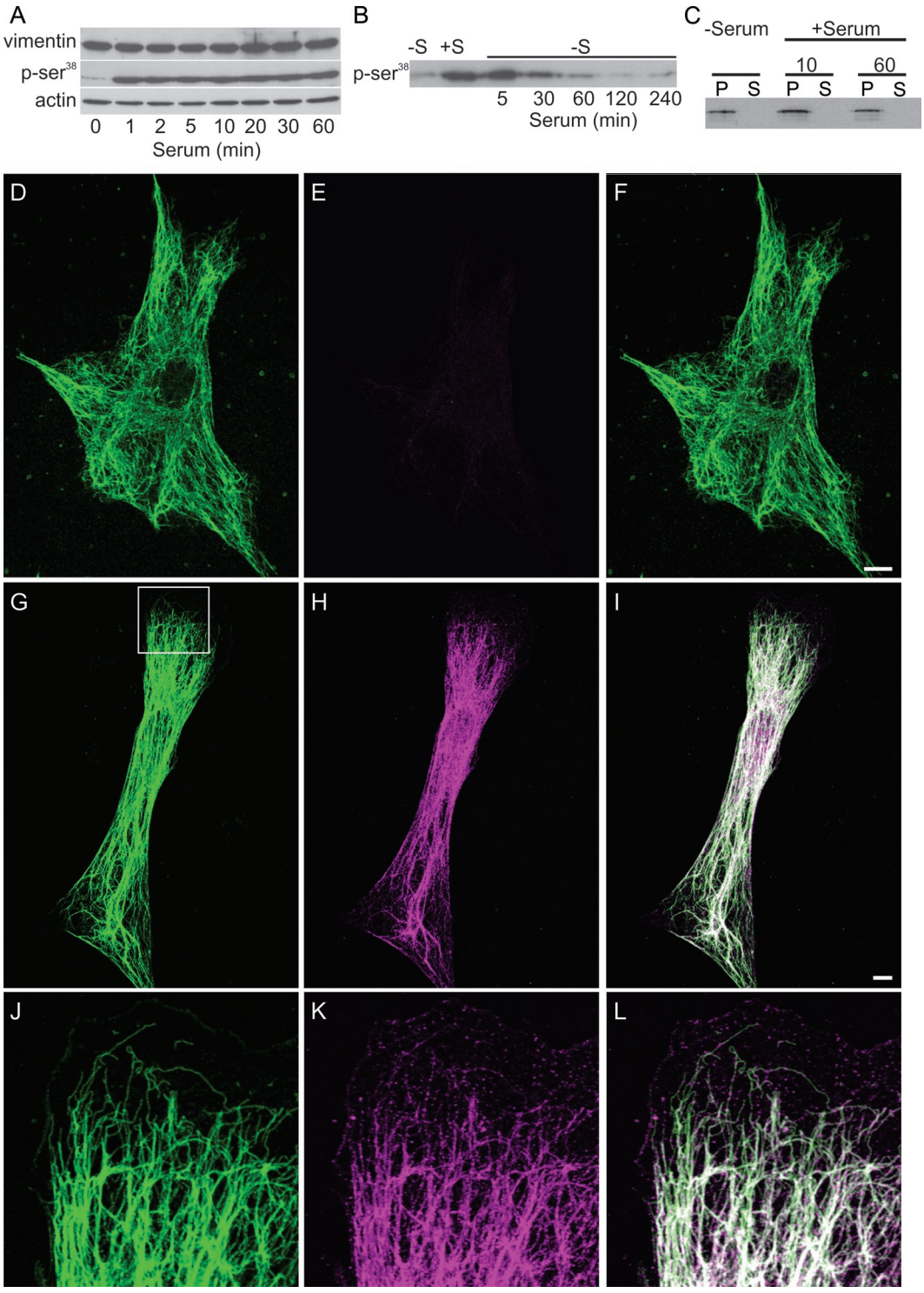

FIGURE 3: Vimentin-Ser phosphorylation increases after serum addition. (A) Immunoblotting demonstrates that phosphorylation of vimentin Ser-38 increases dramatically within 1 min after serum addition and persists up to 60 min. Vimentin and actin are used as loading controls, and the pSer-38 blot has been exposed long enough to show the signal at 0 min. (B) Time course of vimentin–Ser-38 phosphorylation after serum activation followed by serum depletion. Cells were serum starved for 72 h (lane marked −S); serum was added for 30 min (+S), and then cells were replaced into serum-free medium and cell lysates prepared at the indicated times (5–240 min). (C) No differences were detected in the distribution of vimentin between the pellet and supernatant fractions after serum starvation (72 h) or 10 min and 60 min after serum stimulation. (D–F) Double-label immunofluorescence with anti-vimentin (D) and anti–vimentin pSer-38 (E) showing that this residue is minimally phosphorylated in a serum-starved 3T3 cell (72 h; F, overlay). (G–I) Staining with the anti–vimentin pSer-38 in a 3T3 cell 10 min after serum addition. Note that the entire VIF network stains with this phosphospecific antibody (G, anti-vimentin; H, anti–vimentin pSer-38; I, overlay; 10 min). (J–L) Higher magnification of the area denoted by the box in (G) demonstrates that pSer-38 is also found in particles and squiggles in the region where a lamellipodium is formed. Bars = 10 μm.

reaction by immunofluorescence or immunoblotting following serum stimulation (data not shown). Interestingly, even though Ser-38 phosphorylation appears to take place throughout the entire VIF network, the disassembly and retraction of the VIF network takes place only within certain small regions near the cell surface (Figure 3, G–L). This localized VIF disassembly was confirmed by analyses of the pellet and supernatant fractions of IF-enriched cytoskeletal preparations, which revealed no detectable differences in the amount of soluble vimentin following serum addition using either anti-vimentin or anti–pSer-38 (Figure 3C and data not shown; Yoon *et al.*, 1998). Because of this, we sought a technique that would permit us to examine the changes in vimentin assembly states in a more localized and controlled manner, as described later in this article.

Vimentin is reorganized following Rac1 activation

The dynamic properties of VIF during the formation of lamellipodia were determined by taking advantage of a photoactivatable Rac1 (PA-Rac1) that can be used to induce the formation of lamellipodia (Fukata *et al.*, 2003; Wu *et al.*, 2009). Nonirradiated serum-starved fibroblasts expressing PA-Rac1 have no lamellipodia and contain VIF networks that extend to the cell surface (Figure 4, A–D; n = 50). Within 5–10 min of activating PA-Rac1 by exposing entire dishes of serum-starved cells to light, immunofluorescence studies showed that the VIF had withdrawn from the cell surface (Figure 4E) as Arp2/3-enriched lamellipodia became apparent around the entire cell periphery (Figure 4G; n = 50). Vimentin particles are apparent in the lamella and lamellipodial regions of these cells (Figure 4F).

A major advantage of the PA-Rac1 construct is that it can also be activated in a defined subcellular region of a single cell to locally induce the formation of a lamellipodium (Wu *et al.*, 2009). Therefore we photoactivated live, serum-starved 3T3 fibroblasts coexpressing mCherry-PA-Rac1 and Emerald-vimentin. Local activation of PA-Rac1 induced a retraction of the VIF within and near the irradiated area (Figure 4I; see Supplemental Video S2). Interestingly, we found that the number of light pulses required to induce ruffling was dependent on the density of the VIF adjacent to the cell surface. In regions that contained few VIF (see Figure 4I), the induction of lamellipodia required only a single pulse that was coincident with the retraction and disassembly of VIF. In contrast, where there were thick bundles of VIF, between 10–30 pulses were required (Figure 4J; see also Supplemental Video S3). In all instances, the withdrawal of VIF toward the nucleus was accompanied by their disassembly, as indicated by an increased number of squiggles, and some particles in the region vacated by the withdrawing VIF. Detailed observations of bundles of VIF at the cell periphery demonstrated that their retraction was accompanied by their apparent unwinding and loosening, giving rise to thinner fibrils and squiggles, the latter of which subsequently moved away from the bundle (Figure 4J and Supplemental Figure S3). PAK is activated by Rac1 and it phosphorylates vimentin at Ser-38 (Goto *et al.*, 2002). Therefore we determined whether the photoactivation of an entire mEF cell expressing PA-Rac1 would also induce the phosphorylation of vimentin at Ser-38. Immunofluorescence observations of cells transfected with PA-Rac1 revealed a dramatic increase in vimentin pSer-38 staining within 1–2 min of whole-cell PA-Rac1 activation (Figure 5, A–C), while neighboring cells on the same coverslip that were not expressing PA-Rac1 exhibited much less vimentin pSer-38. Vimentin phosphorylation was always observed before obvious membrane ruffling. Quantitative immunoblot analyses of whole-cell extracts obtained from irradiated or nonirradiated mEF cultures stably expressing the PA-Rac1 construct demonstrated an ~400% increase in vimentin pSer-38 within 10 min following exposure to light (Figure 5D).

To gain a better understanding of the spatial relationship between the activation of Rac1 and vimentin phosphorylation, we locally irradiated ~10-µm-diameter spots in PA-Rac1–expressing fibroblasts and looked for changes in vimentin phosphorylation at Ser-38. Immediately after photoactivation, there was a significant increase in the phosphorylation of Ser-38 on the VIF at the site of irradiation (Figure 5, E–H). Fixation within 10–30 s after photoactivation revealed that the area of phosphorylation appeared to be spreading away from the site of irradiation along the vimentin network (Figure 5, I–L). Finally, within 1 min following the irradiation of an ~10-µm-diameter spot, the entire VIF network showed an increase in Ser-38 phosphorylation compared with nonirradiated cells (Figure 5, M–P).

The targeted disassembly of VIF induces the formation of lamellipodia

The results described above suggest that the presence of a VIF network at the edge of a cell inhibits the formation of lamellipodia. To further test this hypothesis, we used a dominant-negative mimetic peptide, 2B2. This peptide is derived from the C-terminal end of the central rod domain (residues 355–412) and has been shown to inhibit the assembly of VIF in vitro (Strelkov *et al.*, 2002). We show here that the 2B2 peptide also drives the disassembly of polymerized VIF in vitro, as determined by negative stain electron microscopy (Figure 6, A–C). This disassembly begins within 10 s following the addition of the 2B2 peptide, resulting in the appearance of short filaments alongside the remaining long VIF (Figure 6B). After 5 min, VIF have been disassembled nearly completely into ULF-like structures, with an occasional short filament (Figure 6C). To determine the effects of the 2B2 peptide on VIF networks in vivo, 3T3 cells were serum-starved for 72 h and then microinjected with the 2B2 peptide and studied by immunofluorescence at time intervals up to 180 min. At concentrations above 5 µg/ml in injection buffer, the microinjection of 2B2 peptide caused cells to round up and detach from the substrate, as we previously reported in the case of the Vim-1A peptide (data not shown; Goldman *et al.*, 1996). However, at a concentration of 2.0 µg/ml in injection buffer, it was obvious that extended VIF networks disappeared from the cell periphery, but some VIF remained in the juxtanuclear region (Figure 6D). In addition, numerous particles remained throughout the cytoplasm and were particularly enriched in the regions at the cell surface where lamellipodia typically formed (Figure 6D, inset). The microinjection of serum-starved cells with a lower concentration of 2B2 (0.5 µg/ml in injection buffer) usually elicited a more local retraction of the VIF from the cell surface, which was coincident with the formation of a lamellipodium near the injection site. Staining with Arp2/3 antibody verified that the lamellipodia were induced in all cells in which the VIF were reorganized (Figure 6E; n = 100). In contrast, microinjection of a scrambled peptide (Figure 6F; n = 20), bovine serum albumin (BSA; n = 50), or buffer alone (n = 50) into serum-starved cells did not alter the overall organization of VIF or induce the formation of lamellipodia. In some cases, microinjected live cells exhibited upper surface ruffles at the injection site (Figure 6, G–I). Under serum-starved conditions, the induction of ruffling following microinjection took ~30–60 min.

We confirmed the effects of the 2B2 peptide on VIF organization and the formation of lamellipodia by microinjecting live Emerald-vimentin–expressing 3T3 cells that had been serum-starved for 72 h (n = 35). As described above, we observed several responses. Some cells began to ruffle around their entire

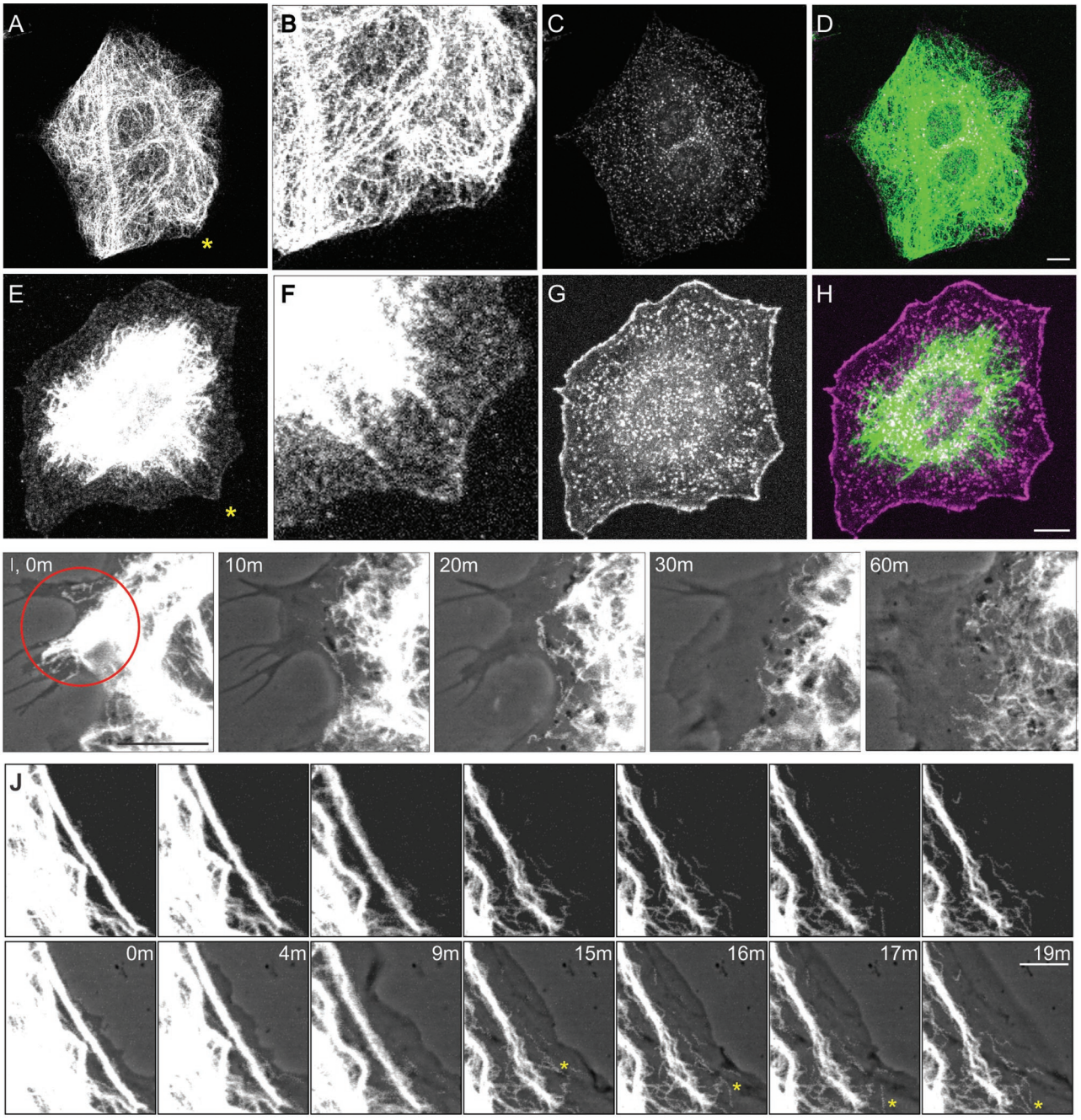

FIGURE 4: PA-Rac1 activation induces vimentin reorganization. (A–D) Double-label immunofluorescence showing that the VIF network extends to the cell periphery in a serum-starved (72 h) mEF stably expressing PA-Rac1 (A, vimentin; B, higher magnification of area near asterisk in A). These cells do not have lamellipodia, as indicated by staining with anti-Arp2/3 (C, Arp2/3; D, overlay). (E–H) Within 10 min after whole-cell irradiation, VIF have withdrawn from the edge of the cell (E, anti-vimentin; F, higher magnification of area near asterisk in E). This retraction is coincident with the formation of lamellipodia that encircle the entire cell as indicated by Arp2/3 staining (G, Arp2/3; H, overlay). Vimentin particles are evident within the lamella and lamellipodium (E, F). Cells were fixed in formaldehyde to preserve the actin-rich structures within the lamellipodia rather than methanol, which is the optimal fixation for vimentin (see *Materials and Methods*). Bars (D, H) = 10 μm. (I) Local activation of Rac1 in a region of a serum-starved (72 h) 3T3 cell expressing both Emerald-vimentin and PA-Rac1. This region contains relatively few VIF, oriented toward the cell surface. Within minutes after a single pulse of irradiation (red circle), local membrane ruffling is initiated (I, phase contrast and Emerald-vimentin overlay at indicated time intervals after irradiation). The VIF network appears to disassemble and retract from the cell surface as the lamellipodium forms (see Supplemental Video S2). (J) Serum-starved (72 h) 3T3 cells stably expressed PA-Rac1 and transiently expressed Emerald-vimentin. Thick bundles of VIF are evident parallel to the edge of the cell. Following the irradiation of only this region, these bundles appeared to unwind and retract from the cell surface. This was coincident with the formation of squiggles and particles, many of which moved rapidly out of the field of view (see asterisk for moving squiggle; also see Supplemental Video S3; top row, fluorescence images taken at the time intervals indicated; bottom row, same images superimposed over phase contrast to show the expanding lamellipodial region). Bars (I, J) = 5 μm.

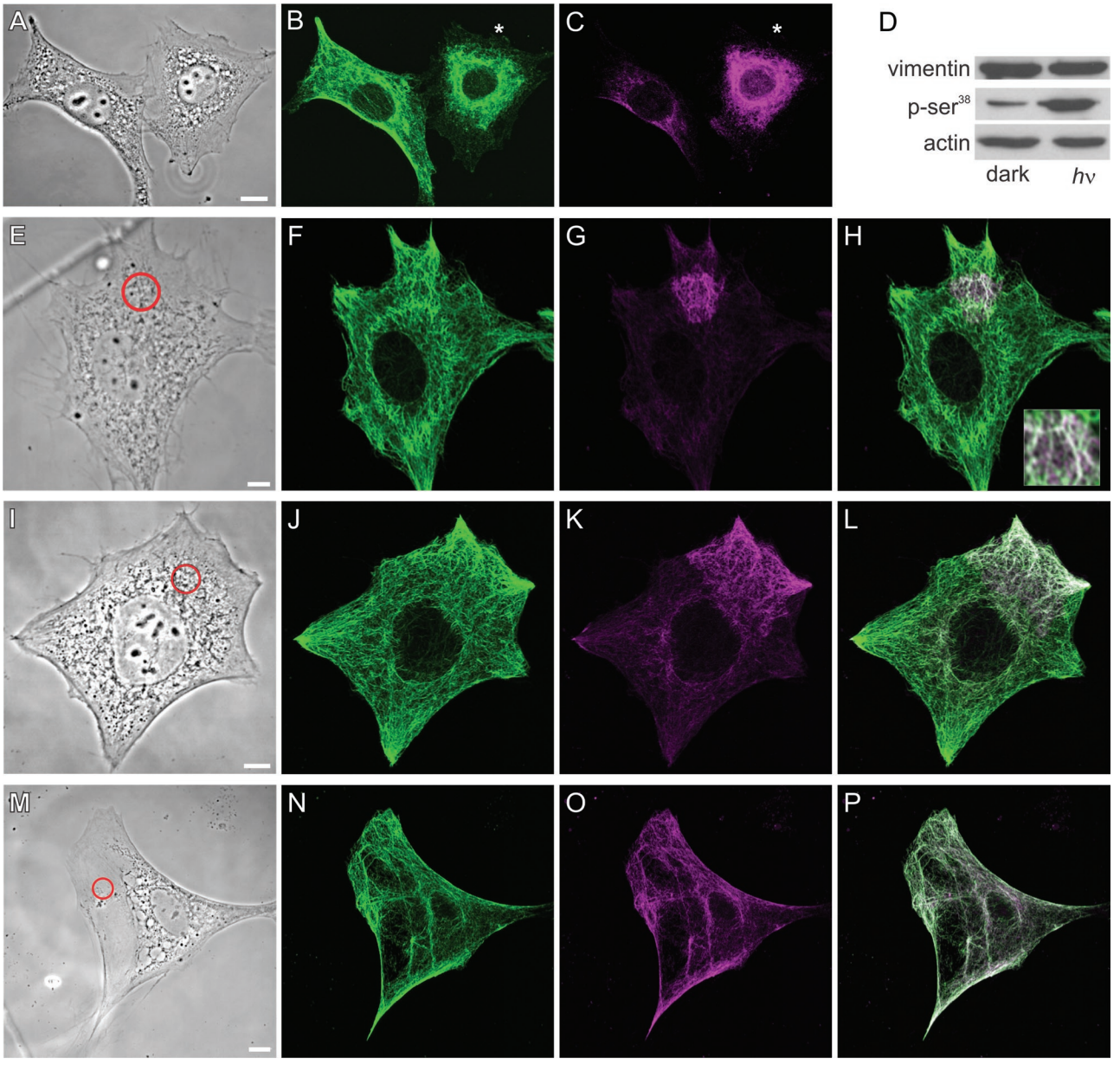

FIGURE 5: Activation of PA-Rac1 induces vimentin-Ser phosphorylation. (A–C) mEF transiently expressing PA-Rac1 were serum starved for 72 h, and then the entire coverslip was irradiated before fixing and staining with antibodies directed against vimentin (B) and vimentin pSer-38 (C). Cells expressing PA-Rac1 were indentified by their mCherry tag (data not shown; cell indicated by asterisk, see *Materials and Methods*). Note that the VIF have retracted from the periphery of the PA-Rac1–expressing mEF (A, B) and that they are phosphorylated at Ser-38 (C). In comparison, the VIF were not reorganized in a neighboring cell that did not express PA-Rac1 (cell without asterisk). Immunoblotting revealed a significant increase in pSer-38 after the irradiation of serum-starved (72 h) cultures of cells stably expressing PA-Rac1 (D, vimentin pSer-38). (E–P) mEF stably expressing PA-Rac1 were also spot irradiated and then fixed and processed for immunofluorescence at the indicated time intervals. In cells fixed immediately after photoactivation, VIF were phosphorylated at Ser-38 in or only near the irradiated area (see red circle; E, phase contrast; F, vimentin; G, vimentin pSer-38; H, overlay; inset shows irradiated region). Within 10–20 s, the area of vimentin pSer-38 had spread from the irradiated spot (I, phase contrast; J, vimentin; K, vimentin pSer-38; L, overlay), and by 45–60 s, vimentin pSer-38 was evident throughout the entire VIF network (M, phase contrast; N, vimentin; O, vimentin pSer-38; P, overlay). Bars = 10 μm.

periphery, and this was coincident with the disassembly and retraction of the entire VIF network toward the nucleus (Figure 7, A and B). In other cells, the local disassembly of the VIF network was coincident with local membrane protrusion (Figure 7, C–J). Subsequent immunofluorescence observations of these same microinjected cells confirmed that these regions contained the parallel actin filaments typical of lamella and lamellipodia (Figure 7, H–J).

We also studied the effects of the 2B2 peptide in cells maintained in 2% serum for 72 h. Cells grown in this low level of serum contain fewer and smaller membrane ruffles than cells maintained in normal serum and have numerous nonruffling, rigid-appearing

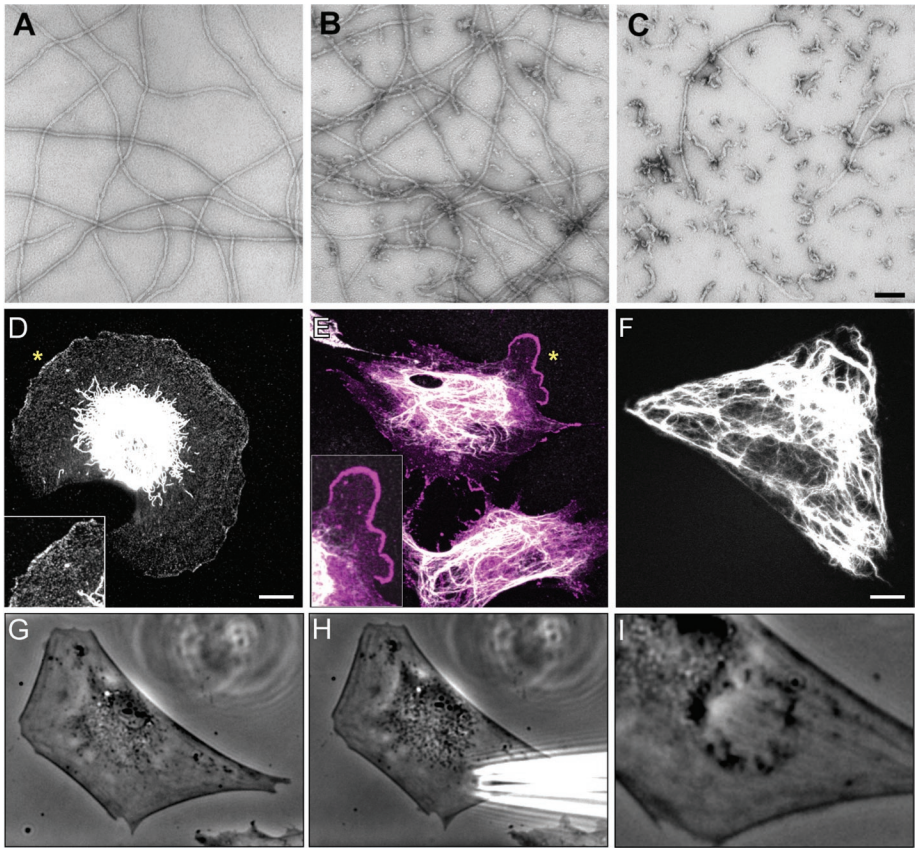

FIGURE 6: The mimetic 2B2 peptide disassembles VIF in vitro and induces ruffling in vivo. (A–C) The addition of the mimetic 2B2 peptide to recombinant human vimentin assembled for 1 h (A) induced depolymerization that began within 10 s after addition (B) and rapidly proceeded so that after 5 min predominantly ULF-like structures remained (C). Negative stain electron microscopy. Bar = 100 μm. (D–F) In response to the microinjection of higher concentrations of 2B2 into serum-starved (72 h) mEF cells, the VIF frequently retracted from the entire cell periphery (D, immunofluorescence with anti-vimentin; inset, higher magnification of region indicated by asterisk). Note the presence of vimentin particles in the region between the retracted VIF and the cell surface, which shows extensive membrane ruffling. This cell was fixed 60 min after microinjection. (E) In cells injected with lower concentrations of peptide and fixed 30–60 min later, the VIF frequently disassembled near the injection site, where lamellipodia also formed, as indicated by Arp2/3 staining (E, double-label immunofluorescence; vimentin, white; Arp2/3, magenta; inset, higher magnification of region near asterisk). In comparison, control serum-starved (72 h) 3T3 cells or mEF that were microinjected with a scrambled peptide, BSA, or buffer alone did not show an altered distribution of their VIF and lamellipodia were not induced (F, GFP-vimentin in a live 3T3 cell after the injection of scrambled peptide). (G–I) Occasionally, upper surface ruffles were apparent after the microinjection of 2B2 at the injection site (G, H, live 3T3 cell before; I, 10 min postinjection). Bars = 10 μm.

regions at their edges. Cells maintained in 2% serum also responded much more rapidly to the 2B2 peptide (0.5 μg/ml in injection buffer), as evidenced by the formation of lamellipodia within ~10 min following microinjection. This enabled us to monitor the behavior of microinjected cells for longer periods of time. For these experiments, cells were injected at sites near the nonruffling, rigid-appearing regions. In 36% of the cells (n = 22), a ruffled membrane formed primarily near the microinjection site. In some cases, motile cells reversed direction and moved toward this newly formed lamellipodium (Figure 8, A–H, arrow denotes site of injection). In ~45% of the microinjected cells, ruffling was induced around the entire cell periphery (e.g., Figure 7B). The remaining ~22% of the microinjected cells rounded up, and many of them subsequently respread and exhibited circumferential membrane ruffling (data not shown). A few of these rounded-up cells detached from the substrate, which is similar to the behavior of cells following the microinjection of other vimentin peptides (Goldman *et al.*, 1996).

Alterations in VIF decrease the rates of cell motility

As shown above, the majority of fibroblasts exhibit extended VIF networks and very little lamellipodial activity when grown in the absence of serum. As a further test of the role of VIF in inhibiting the formation of lamellipodia, we examined vim$^{-/-}$ mEF. We found that after incubation in serum-free medium for up to 72 h, vim$^{-/-}$ mEF continued to form lamellipodia (as indicated by Arp2/3 staining) at a significantly greater frequency than did normal (vim$^{+/+}$) mEF grown under the same conditions (Figure 9, A–C: vim$^{-/-}$, 57.2 ± 4.0% vs. D–F: vim$^{+/+}$, 20.6 ± 1.1% after 72 h, n = 100, $p < 0.01$). Because lamellipodia are the major locomotory organelles of fibroblasts, we also determined the effect of the presence or the absence of VIF on cell migration. Previous support for a role for VIF in cell motility comes from findings of impaired locomotion in mEF obtained from vim$^{-/-}$ mice (Eckes *et al.*, 1998; Mendez *et al.*, 2010). To provide further support for the role of VIF in cell motility, we characterized the behavior of fibroblasts expressing the dominant-negative GFP-vimentin$_{(1–138)}$ construct, which alters the normal assembly of VIF networks (Kural *et al.*, 2007; Chang *et al.*, 2009). Within 24 h following transfection, these cells exhibited membrane ruffling around their entire peripheries, but their locomotory behavior was severely impaired (Figure 10, A and B; see Supplemental Video S4; GFP-vimentin(1–138), 0.008 ± 0.004 μm/s vs. controls, 0.020 ± 0.006 μm/s; n = 42; $p < 0.001$). The formation of lamellipodia was confirmed in these cells by immunofluorescence using antibodies directed against actin, Arp2/3, and cortactin (data not shown). We also determined the effect of vimentin silencing on rates of cell motility in 3T3 cells. Immunoblot analyses of 3T3 cells expressing vimentin short-hairpin RNA (shRNA) showed a 75% reduction in vimentin expression (data not shown). These cells exhibited membrane ruffling around their entire peripheries, similar to vim$^{-/-}$ mEF (Mendez *et al.*, 2010), and the motility of these cells was significantly reduced (Figure 10, C and D; n = 30, 0.009 ± 0.005 μm/s) compared with controls (Figure 10, E and F; n = 30, 0.030 ± 0.009 μm/s; $p < 0.001$). Taken together, these data confirm that an organized VIF network is required for fibroblast motility but not for the formation of lamellipodia.

DISCUSSION

VIF inhibit the formation of lamellipodia

Our results demonstrate that there are gradients of the different assembly states of vimentin in migrating fibroblasts, as indicated by a high concentration of VIF within the tail and perinuclear regions, a

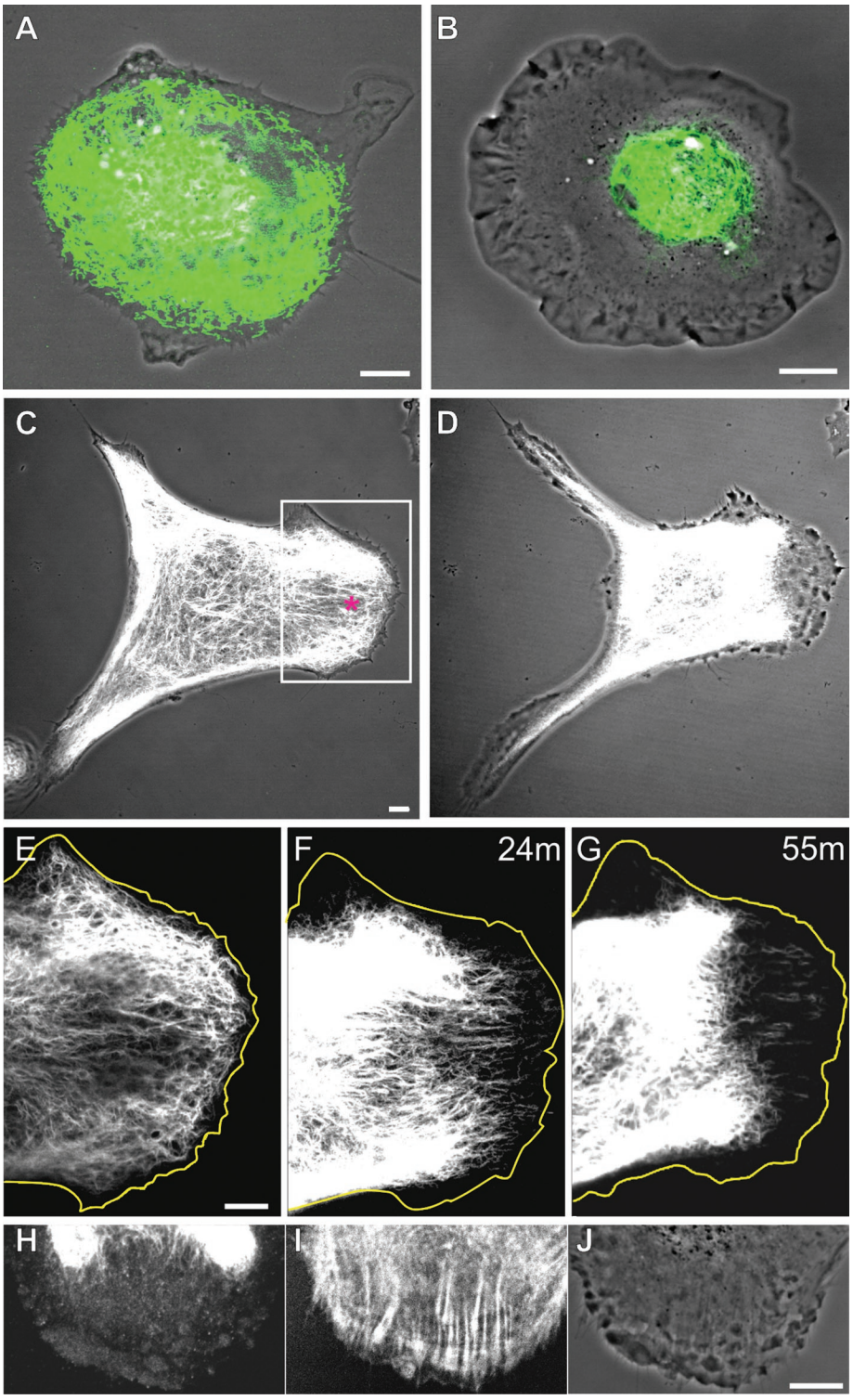

FIGURE 7: Live imaging of the disassembly of VIF and membrane ruffling. (A–B) A live mEF expressing Emerald-vimentin and maintained in 2% serum was microinjected with 2B2 peptide. Following microinjection, the VIF network disassembled and withdrew from the cell periphery, and this was coincident with lamellipodial activity over most of the cell surface (A, Emerald-vimentin and phase contrast overlay, before; B, 10 min after microinjection). (C–J, images of the same cell, C–G, live; H–J, fixed) Emerald-vimentin in a live, serum-starved (72 h) 3T3 cell with an extended VIF network (C, Emerald-vimentin and phase contrast overlay, before injection; asterisk indicates injection site). Within ~30 min, the VIF network began to disassemble near the site of microinjection (E, region indicated by box in C), and VIF disassembly continued as membrane ruffles formed near the injection site. Squiggles were also present in these regions (F, G, vimentin; indicated times are postmicroinjection; D, 60 min after microinjection). The subsequent fixing and staining of the same microinjected cell confirmed that vimentin particles were also present within the newly formed lamella and lamellipodia (H, vimentin; I, F-actin; J, phase contrast). All bars = 10 μm.

relative decrease in long VIF and increase in squiggles (short IF) and nonfilamentous particles within the lamella, and an enrichment of particles within the lamellipodium. Thus the distributions of the different assembly states of vimentin are correlated with the shape and polarity of locomoting cells. In support of these observations, it has previously been shown that vimentin plays a dominant role in the shape transitions and increased motility of cells undergoing the EMT (Hendrix *et al.*, 1997; Mendez *et al.*, 2010). Other evidence has been derived from the microinjection of the mimetic vimentin 1A helix initiation peptide, which disassembles VIF mainly into monomers and dimers, causing fibroblasts to completely round up and lose their substrate attachments (Goldman *et al.*, 1996). In addition, silencing other type III IF proteins such as glial fibrillary acidic protein and peripherin cause significant shape changes in astrocytoma and PC12 cells, respectively (Weinstein *et al.*, 1991; Helfand *et al.*, 2003).

In this study, we show that the mimetic vimentin peptide, 2B2, disassembles VIF into ULF, rather than the lower order structures resulting from the 1A peptide experiments (Goldman *et al.*, 1996). Low concentrations of 2B2 microinjected into serum-starved fibroblasts frequently caused VIF to disassemble and retract from the edge of the cell near the injection sites where lamellipodia formed. At higher concentrations, the 2B2 peptide frequently caused more extensive VIF disassembly and retraction, and it induced membrane ruffling around the entire cell surface. In similar experiments, peripheral nonruffling regions of fibroblasts grown in 2% serum were induced to ruffle by 2B2 microinjection, and subsequently these cells changed their direction of translocation. These results demonstrate that the targeted disassembly and retraction of the VIF network from the cell perimeter can induce membrane ruffling and alter cell movement.

Our results also show that locomotion is inhibited in $vim^{-/-}$ cells, vimentin-silenced cells, and cells expressing the dominant-negative $vimentin_{(1–138)}$, even though under each of these experimental conditions cells ruffle extensively around their entire perimeters, indicating that VIF play a role in cell

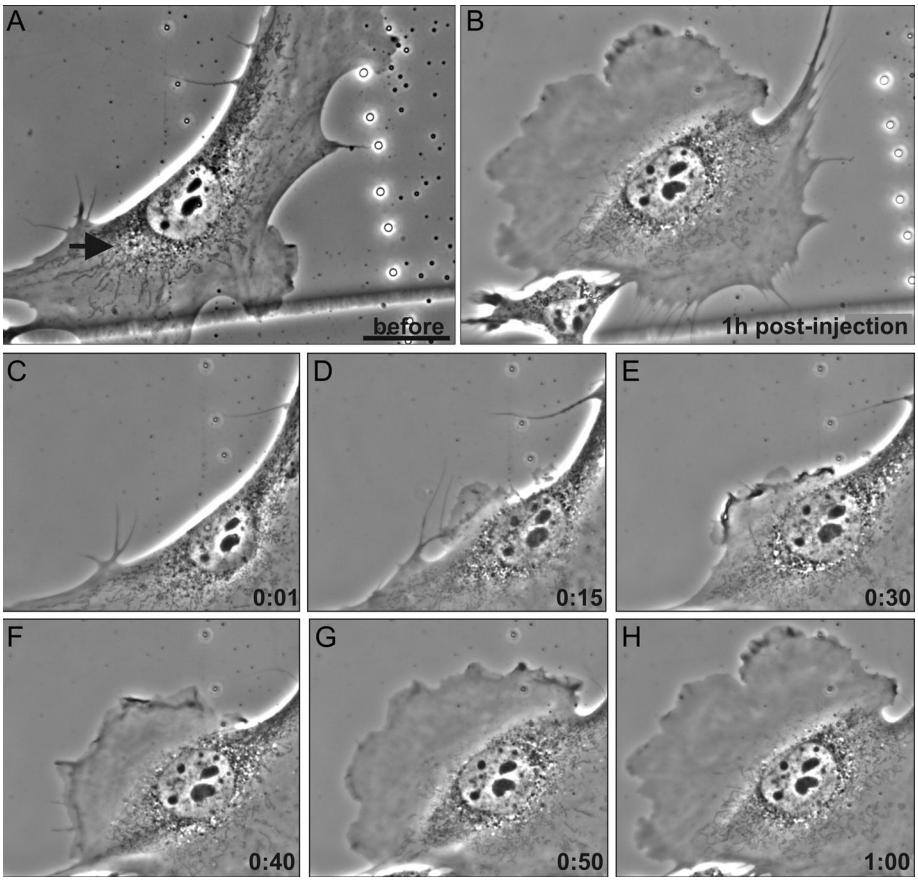

FIGURE 8: Live imaging of altered motility following VIF disassembly in 2B2-microinjected serum-deprived cells. (A–H, live phase contrast images of the same cell). Moving mEF cells maintained in 2% serum were microinjected with 2B2 opposite ruffling areas (A, arrow marks the microinjection site). Small membrane protrusions became apparent near the site of microinjection within ~10 min (D, 15 min). This lamellipodium became more prominent with time, and eventually this cell began to move in the direction of the newly formed lamellipodium (A–H, note the retraction fibers above the cell in A and below it in B; see Supplemental Video S4). Bar = 100 μm.

motility. This inhibition of motility in the absence of normally organized VIF may be related to the inability of the affected fibroblasts to establish the polarity required for motility. Thus the regulation of the disassembly of VIF may act as a molecular clutch that modulates the actin-based machinery responsible for moving cells. In contrast, when VIF are polymerized subjacent to the cell surface, they act as a brake and a mechanical stabilizer to inhibit the formation of lamellipodia.

IFs as mechanical stabilizers in the regulation of cell locomotion

In support of their role as mechanical stabilizers of the cell surface, VIF have been shown to withstand significantly greater mechanical stresses in vitro than either microtubules or microfilaments, and they also exhibit strain hardening properties and can be stretched to ~3× their length (Janmey *et al.*, 1991; Kreplak *et al.*, 2005, 2008). These characteristics are inherent in all types of cytoplasmic IF proteins (Lin *et al.*, 2010). In vivo support for their mechanical roles is derived from the fact that mutations in keratin IF proteins have been associated with blistering diseases of the skin, in which keratinocytes become fragile and prone to rupturing upon mild physical stress (Chan *et al.*, 1994). It has also been demonstrated that the organization of IF networks rapidly changes in response to shear forces (Helmke *et al.*, 2000; Sivaramakrishnan *et al.*, 2008). For example, shear induces changes in the mesh size of the keratin IF network, resulting in an increase in its stiffness, further demonstrating that the IF network provides cells with a mechanism to withstand external mechanical forces (Sivaramakrishnan *et al.*, 2008). It is likely that the flexibility and strain-hardening properties of IF could locally control the stiffness of regions of a cell, thereby acting as determinants of the location and positioning of lamellipodia.

The local regulation of cell stiffness by VIF may help to explain the behavior of locomoting fibroblasts. In Abercrombie's (1961) original descriptions of the properties of ruffled membranes in moving fibroblasts, he observed that a leading lamellipodium frequently stops ruffling as a new ruffle forms elsewhere on the cell surface, thereby causing the cell to move in a different direction. Little is known regarding the factors that determine the site of the formation of a lamellipodium. Certainly, this involves a series of complex interactions between external stimuli (e.g., growth factors), cell surface receptors, internal signaling pathways (e.g., Rho and Rac), and the reorganization of the cytoskeletal systems and their associated proteins. On the basis of our results, we hypothesize that the local organization of VIF participates in the determination of these sites. In support of this, we found that regions containing relatively few VIF could be induced to ruffle by significantly less PA-Rac1 activation than was necessary in regions containing more VIF. These results may explain the previous observation that some cellular regions required much greater irradiation than others to initiate lamellipodia following PA-Rac1 activation (Wu *et al.*, 2009).

Vimentin phosphorylation and the regulation of IF assembly and organization

The functional significance of the finding that there is an enrichment of nonfilamentous vimentin particles within newly formed lamellipodia is unknown. These structures have been shown to be precursors in the assembly of short IF (squiggles; Prahlad *et al.*, 1998). Similar precursors to keratin IF have been reported in the peripheral regions of epithelial cells (Windoffer *et al.*, 2006). While the exact origin of the vimentin particles remains to be determined, it is likely that at least some of these structures arise from the disassembly of preexisting VIF. This disassembly is probably regulated by protein kinases (e.g., Lamb *et al.*, 1989), as it has been shown that phosphorylation plays a critical role in regulating the assembly states of VIF. For example, phosphorylation of Ser-55 in the non–α-helical N-terminal domain of vimentin by Cdk1 is responsible for VIF disassembly into nonfilamentous particles as cells round up to enter mitosis (Chou *et al.*, 1990). However, the determination of the relevance of phosphorylation during the induction of ruffling is complex, as vimentin has 53 known and putative phosphorylation sites (Li *et al.*, 2002;

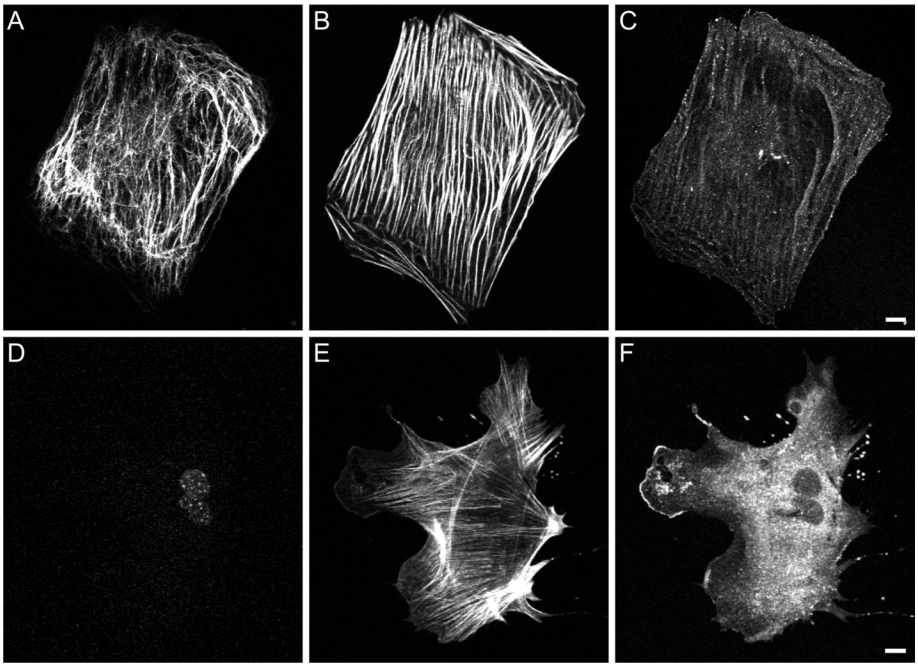

FIGURE 9: Lamellipodia are active in serum-starved vimentin mEF. (A–C, triple-label immunofluorescence of serum-starved [72 h] mEF). The majority of VIF in serum-starved $vim^{+/+}$ mEF extend to the cell edges (A, vimentin). In these cells, thick stress fibers formed (B, actin), and lamellipodia were evident in only ~20% of the cells, as indicated by Arp2/3 staining, even after 72 h (C, Arp2/3). (D–F triple-label immunofluorescence of serum-starved [72 h] $vim^{-/-}$ mEF) In contrast, ~60% of serum-starved vimentin-null mEF continued to form Arp2/3-enriched lamellipodia in the absence of serum (D, vimentin; E, F-actin; F, Arp2/3). Bars = 10 μm.

Consortium, 2010). Of these, 19 sites reside in the N-terminus, a domain that is known to play an important role in the polymerization of IF (Chou *et al.*, 1991, 1996; Herrmann *et al.*, 1996). Many of these sites are targets of kinases that are involved in the induction of lamellipodia and cell motility. These include PI3Kγ (Barberis *et al.*, 2009), ROKα (Sin *et al.*, 1998), PKC (Inagaki *et al.*, 1987), Raf-1 (Janosch *et al.*, 2000), protein kinase A (Howe, 2004), PAK (Goto *et al.*, 2002), and AKT1 (Zhu *et al.*, 2011). Vimentin Ser-38 is a particularly interesting site because it is targeted by at least seven kinases, including PAK, PKCε, and AKT (Ando *et al.*, 1989; Izawa and Inagaki, 2006; Zhu *et al.*, 2011). The latter three are known to be activated by Rac1 or serum addition. Using an antibody directed against vimentin pSer-38, we show that there is an ~350–400% increase in phosphorylation at this site coincident with the induction of membrane ruffling. This is accompanied by both the local disassembly of VIF near the cell surface and an increase in the rate of subunit exchange along the remaining VIF as indicated by FRAP analysis. Interestingly, the local photoactivation of PA-Rac1 within an ~10-μm-diameter spot is associated with an immediate increase in Ser-38 phosphorylation only within the illuminated area. This local phosphorylation is rapidly propagated along the VIF network throughout the cell in <1 min. Yet under these experimental conditions, we can detect the disassembly and retraction of VIF adjacent to the cell surface only near the initial site of PA-Rac1 activation.

A possible explanation for the local disassembly of VIF during the formation of lamellipodia could be related to the levels of vimentin phosphorylation. For example, the conversion of VIF into the particles and squiggles seen subjacent to ruffles may require a higher level of phosphorylation than that necessary to induce subunit turnover in the remainder of the VIF network. Our FRAP data following serum addition suggest that this could be the case, as we demonstrate a twofold increase in the rate of subunit exchange in the VIF networks retained in regions not associated with the ruffled membrane. Other factors complicating our understanding of the regulation of VIF assembly states are the large number of kinases known to interact with vimentin, the regulation of the numerous kinase/phosphatase equilibria involved in regulating the dynamic properties of VIF, and the number of posttranslationally modified residues in the vimentin protein chain. It is also possible that, following the phosphorylation of one site, additional sites become more accessible and therefore more likely to be phosphorylated. In this manner, it is likely that multiple levels of regulation contribute to the state of vimentin assembly. To begin to determine the role of specific phosphorylation sites, we have initiated preliminary experiments into the effect of serum addition to serum-starved, vimentin-null cells expressing networks of a nonphosphorylatable mutant vimentin (S38A). To date, we have not detected an obvious alteration in the overall response to serum addition relative to controls (data not shown). This preliminary result suggests that future studies using the mutagenesis of multiple sites will be required to determine the role of phosphorylation in regulating the dynamic properties of VIF, their disassembly and retraction during the formation of lamellipodia.

It should be noted that some particles present within lamellipodia may represent newly synthesized protein. Support for this possibility comes from the presence of vimentin mRNA within the leading edge of cells (Lawrence and Singer, 1986) as well as the finding that vimentin particles are frequently associated with mRNA engaged in the process of "dynamic cotranslational assembly" (Chang *et al.*, 2006). Furthermore, these nonfilamentous particles may have functions distinct from those of fully polymerized VIF. For example, it has been shown during axonal regeneration that newly synthesized, unpolymerized vimentin forms a complex with activated MAP kinase, importin-ß, and cytoplasmic dynein before transport to the nucleus and the subsequent modulation of gene expression (Perlson *et al.*, 2005). It is also possible that the various vimentin structures present in the lamella/lamellipodial regions could be involved in the modulation of focal adhesions during cell motility. In support of this, vimentin has been associated with the distribution of β3 integrin–containing focal complexes (Bhattacharya *et al.*, 2009), the regulation of β1 integrins (Kim *et al.*, 2010), and the rate of turnover of paxillin, an "adaptor protein" common to all focal adhesions (Mendez *et al.*, 2010). Finally, we hypothesize that at least a subpopulation of these particles represents a storage form for the assembly of VIF networks that act to mechanically stabilize the spreading cytoplasm as a fibroblast moves forward in the direction of the leading lamellipodium.

CONCLUSIONS

This study defines a role for vimentin in the regulation of lamellipodium formation and cell motility. Specifically, when networks of VIF are assembled and associated with the cell surface, membrane ruffling and the formation of lamellipodia are inhibited. Conversely,

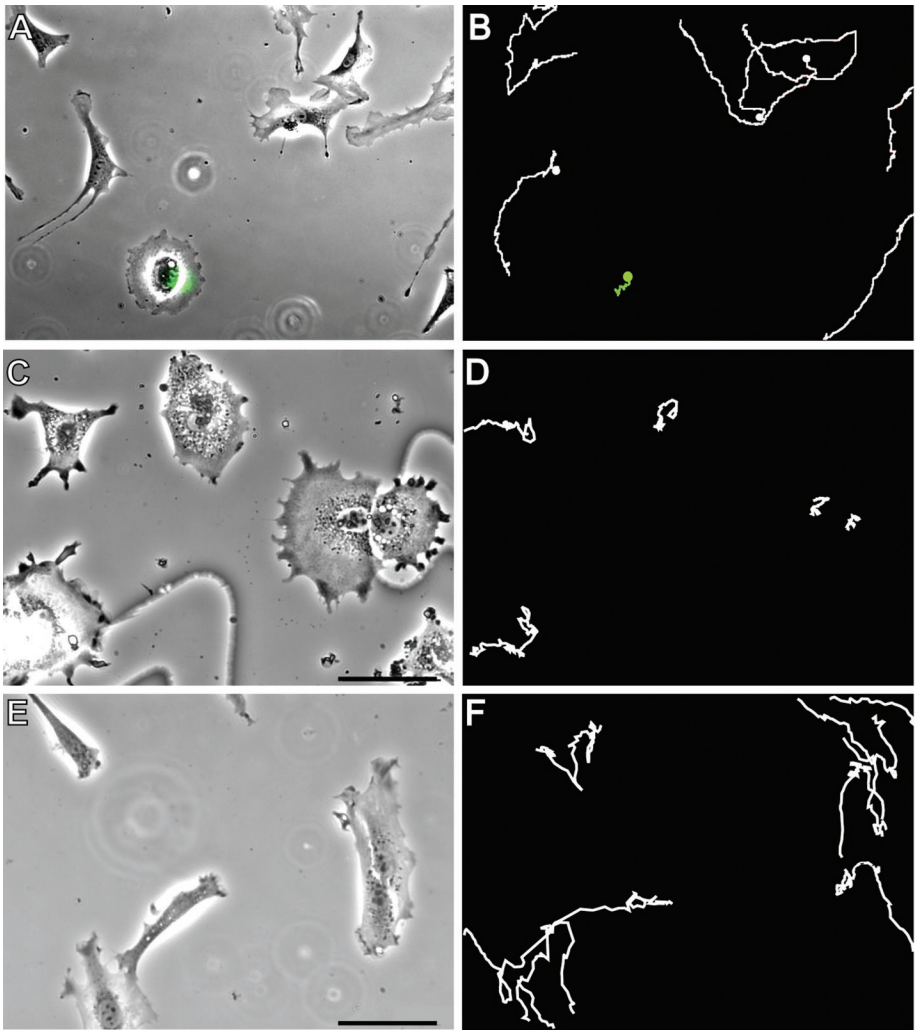

FIGURE 10: An organized vimentin network is required for cell motility. Fibroblasts expressing the dominant-negative vimentin mutant GFP-vim lose their forward/rearward polarity (A, $vim^{+/+}{}_{(1–138)}$ mEF; note GFP signal indicative of GFP-vim expression in the circularly shaped cell). These (1–138)-expressing cells exhibit continuous, circumferential ruffles but do not translocate (B, see green cell path tracing >7 h; see also Supplemental Video S5). In comparison, mEF cells not expressing the dominant-negative mutant maintained their elongated shapes and motility (B, white cell path tracings). Similarly, motility was inhibited in 3T3 cells stably expressing vimentin shRNA (C, D), in contrast to 3T3 cells stably expressing a scrambled sequence (E, F). Bars = 100 μm.

the regulated disassembly of VIF into their structural building blocks allows lamellipodia to form. By modulating the formation of lamellipodia, VIF participate in the regulation of cell polarity and motility.

MATERIALS AND METHODS

Cell culture

NIH-3T3 mouse fibroblasts were maintained in DMEM supplemented with 10% fetal calf serum (FCS) as previously described (Goldman *et al.*, 1992). mEF were isolated from wild-type or vimentin-null mice (obtained from Karen Ridge, Northwestern University, Chicago, IL; Colucci-Guyon *et al.*, 1994) and cultured in DMEM containing 10% FCS as described. mEF stably expressing Tet-inducible (Clontech, Mountain View, CA) mVenus-tagged PA-Rac1 were maintained in DMEM supplemented with 10% FCS, 20 ng/ml puromycin (Sigma, St. Louis, MO), and 1 ng/ml doxycycline (BD Biosciences, Rockville, MD) in order to select for PA-Rac1–expressing cells and to suppress protein expression, as previously described (Wu *et al.*, 2009). These cells were incubated in doxycycline-free medium for 24 h to induce PA-Rac1 expression before the initiation of experiments. NIH-3T3 cells stably expressing vimentin shRNA (discussed later in this article) or a scrambled shRNA control were maintained in medium containing 20 ng/ml puromycin. For serum deprivation and starvation experiments, cells were incubated in DMEM containing 0% or 2% serum for 24–72 h. All of the experiments described in this article were performed in both 3T3 and mEF cells, with the exception of experiments involving stably transfected cells (e.g., mEF expressing PA-Rac1 and 3T3 cells expressing vimentin shRNA).

Antibodies and drug treatments

Antibodies used were rabbit polyclonal anti–vimentin 314 (Helfand *et al.*, 2003), chicken polyclonal anti-vimentin (Covance, Princeton, NJ), rat monoclonal TM38 anti–vimentin pSer-38 (Kosako *et al.*, 1999), rabbit polyclonal anti-VASP (Enzo Life Sciences, Plymouth Meeting, PA), rabbit polyclonal anti-cortactin (Millipore, Billerica, MA), and rabbit polyclonal anti–Arp2 p34 protein (Millipore). Secondary antibodies included FITC-, lissamine-rhodamine–, and Cy5-conjugated goat anti–mouse and anti–rabbit immunoglobulin G (Jackson ImmunoResearch, West Grove, PA), and peroxidase-conjugated goat anti–mouse and anti–rabbit secondary antibodies (Jackson ImmunoResearch) were used for immunoblotting. Immunoelectron microscopy was performed as previously described (Helfand *et al.*, 2002). Fluorophore-conjugated phalloidin (Invitrogen, Carlsbad, CA) was used in some experiments. For other experiments, cells were serum starved for 72 h before exposure to 2 μM nocodazole (Sigma) for 2 h, 2 μM cytochalasin B (Sigma) for 1 h, or 0.1 μM latrunculin B (Sigma) for 1 h before serum addition.

Immunofluorescence

Cells were processed for immunofluorescence using either methanol (−20°C) or 3.7% formaldehyde (room temperature) as previously described (Prahlad *et al.*, 1998; Yoon *et al.*, 1998). Methanol fixation is optimal for visualization of vimentin, whereas formaldehyde fixation was used to preserve actin structures. To determine whether or not a lamellipodium was present, cells were stained for actin and actin-associated proteins using phalloidin and anti-arp2/3. Immunostained preparations were imaged using a Zeiss Confocal LSM510 microscope equipped with a 1.4–numerical aperture (NA) 63× and a 1.4-NA 100× objective (Carl Zeiss, Jena, Germany).

SDS–PAGE and immunoblotting

For SDS–PAGE of total cell protein, cells were grown on 100-mm dishes to ~70% confluence, washed twice with phosphate-buffered saline (PBS) before addition of 1 ml Laemmli sample buffer, and then collected with a rubber policeman and boiled for 5 min. To compare

the proportion of soluble to insoluble vimentin protein, IF-enriched cytoskeletons were prepared as described previously (Helfand *et al.*, 2002) and analyzed for vimentin by immunoblotting at various times following serum replacement. Cells were counted and then lysed in buffer containing 0.5 M KCl, 1% Tx-100, 10 mM $MgCl_2$, a phosphatase inhibitor (1 mg/ml phenylmethylsulfonyl fluoride; Sigma), and protease inhibitors (1 mg/ml TAME [*N*α-(*p*-toluene sulfonyl)-L-arginine methyl ester], Sigma; and Complete EDTA-free, Roche, Indianapolis, IN) in PBS. The lysates were then centrifuged at 1500 × g for 10 min. Samples containing lysate from equal numbers of cells were separated on 7.5% or 10% polyacrylamide gels and transferred to nitrocellulose membranes before immunoblotting with horseradish peroxidase–conjugated secondary antibodies and visualization using enhanced chemiluminescence (Thermo Scientific, Rockford, IL; Helfand *et al.*, 2002). The protein band intensities were quantified using Kodak Molecular Imaging Software v4.0.3 and data analyzed using Microsoft Excel.

Constructs and transfection

Plasmid enhanced GFP (pEGFP)–vimentin (Yoon *et al.*, 1998), vimentin mutant S38A (Eriksson *et al.*, 2004), and the dominant-negative pEGFP-$vim_{(1–138)}$ (Kural *et al.*, 2007) cDNAs were prepared as previously described. Emerald-vimentin was kindly provided by Michael Davidson (Florida State University, Tallahassee). mCherry-PA-Rac1 was prepared as described (Wu *et al.*, 2009). In some experiments, cells were transfected with both Emerald-vimentin and mCherry-PA-Rac1 by electroporation and then plated on coverslips and processed for immunofluorescence within 24–72 h. In other experiments, cells were transfected using FuGene 6 (Roche). In serum starvation and deprivation experiments, transfected cells were placed in normal medium for 6–12 h before incubation in medium containing 0% or 2% serum. Vimentin shRNA (T3; GAATGGTACAAGTCCAAGT; Mendez *et al.*, 2010) and scrambled sequence controls were inserted into the pSilencer5.1 H1 (Clontech) retroviral vector according to the manufacturer's instructions. Briefly, virus was produced by coinfecting equal amounts of the shRNA vimentin T3 pSilencer5.1 H1 construct and pCL-Eco helper plasmid (Imgenex, San Diego, CA) into 293FT cells (Invitrogen) using Xfect Transfection Reagent (Clontech). Culture supernatant was collected on the second day postinfection and incubated with the target cells for 4–8 h in the presence of 8 μg/ml polybrene (Sigma). Two days after infection, cells were placed under 2 μg/ml puromycin selection. Confirmation of vimentin silencing was accomplished by immunoblotting and immunofluorescence.

In vitro analyses of the inhibition of IF assembly by the vimentin 2B2 peptide

Recombinant human vimentin and peptide corresponding to the vimentin 2B2 fragment of the central rod domain (referred to as the 2B2 peptide) were prepared as previously described (Strelkov *et al.*, 2002). Briefly, full-length cDNA was used as a template for PCR amplification, and the amplified products were ligated into the prokaryotic expression vector pPEP-T24 before expression of the construct in BL21(DE3) *Escherichia coli* cells (EMD Biosciences, San Diego, CA). The 2B2 peptide was liberated from the fusion product by thrombin cleavage, purified as described, and dialyzed into 5 mM Tris-HCl buffer, pH 8.4 (Strelkov *et al.*, 2002). The effects of the 2B2 peptide on vimentin assembly into IF were assessed by incubating recombinant vimentin with the peptide at molar ratios ranging from 1:1 to 1:10 (wild-type: 2B2). Formation of VIF was initiated by the addition of assembly buffer (200 mM Tris-HCl [pH 7.0] and 1.6 M NaCl) before samples were incubated at 37°C for times between 10 s and 1 h (Herrmann *et al.*, 1996). In other experiments, VIF were assembled for 1 h before the addition of the 2B2 peptide at molar ratios 1:≤10. Ultrastructural analysis of negative-stained preparations and specific viscosity measurements were evaluated at times intervals up to 70 min, following the initiation of IF assembly or disassembly, as previously described (Herrmann *et al.*, 1993).

Microinjection

Cells grown on locator coverslips (Bellco, Vineland, NJ) were selected for microinjection using either a Zeiss Confocal LSM510 or a Nikon TE-2000 inverted microscope. In some cases, cells were transfected with Emerald-vimentin before microinjecting either the 2B2 peptide, BSA, or a scrambled peptide (Moir *et al.*, 1991) as previously described. Before microinjection, 2B2 or scrambled peptides were dialyzed into microinjection buffer (20 mM Tris, pH 7.5, in 75 mM NaCl) and further diluted to final concentrations of 0.5–10.0 μg/ml (Prahlad *et al.*, 1998). The microinjected cells were either fixed and processed for immunofluorescence within 5–60 min postinjection or imaged live using either a Nikon TE-2000 or Zeiss LSM 510 microscope (detailed later in this article).

Live cell imaging

Time-lapse observations were made at 37°C using either the Zeiss LSM 510 confocal microscope equipped with an airstream stage incubator (Nevtek, Williamsdale, VA; Yoon *et al.*, 1998) or the Nikon Eclipse TE2000-E microscope equipped with the Perfect Focus system (Nikon, Melville, NY) and the INU stage incubator system (Tokai Hit, Shizuoka-Ken, Japan). Images of live cells were captured on the LSM510 at ~3–180-s intervals at a resolution of 512 × 512 pixels per inch with a scanning time of ~1 s for 5–60 min. FRAP was performed as described previously (Yoon *et al.*, 2001). Phase-contrast images of cells were taken simultaneously to ensure that there were no significant changes in cell shape or position during FRAP experiments. Bar-shaped regions were bleached using the line-scan function at 488 nm (100% power, 1% attenuation), and recovery of fluorescence was monitored at 1–2-min intervals for up to 30 min. For experiments conducted on the Nikon microscope, images were captured every ~30–300 s for periods up to 12 h.

The cells expressing PA-Rac1 were maintained and prepared for imaging in the dark or in red light, as described elsewhere (Wu *et al.*, 2009). Briefly, differential interference contrast images were acquired with a red filter (Schott RG610) between the halogen light source and the samples to prevent unintended photoactivation. To activate PA-Rac1, cells were illuminated using a 5-mW LSM 510 Laser Module at 458 nm. Control illumination, which should not activate PA-Rac1, was provided by the 15-mW, 633-nm laser of the same module. Illumination consisted of 1–30 pulses of light using 100% laser power. In some experiments, images of Emerald-vimentin–expressing 3T3 cells were captured every ~10–30 s or every 5–10 min after PA-Rac1 activation to monitor cells for longer time periods. Images were captured using a 1.4-NA 63× or a 1.4-NA 100× objective. Other experiments involved methanol fixation at short time intervals following local irradiation of an ~10-μm-diameter spot. For some experiments, irradiation of entire coverslips was accomplished by exposing the coverslip to fluorescent lighting for 10 min.

Quantitation of cellular motility

The rates of motility of mEF cells expressing dominant-negative vimentin (pEGFP-$Vim_{(1–138)}$) or control cells were determined by live cell imaging. MetaMorph v7.0 (Molecular Devices, Sunnyvale, CA) was used to determine the rate of cell motility using the center of

the nucleus as a reference point that was tracked over time. The distance between these points was determined and then divided by the total time of live imaging to determine velocity. A Student's *t* test was performed to compare the motile properties of cells. Results were considered significant at $p < 0.05$.

Electron microscopy

Cells grown on coverslips were extracted with PEM buffer (100 mM PIPES, pH 6.9, 1 mM MgCl2, 1 mM EGTA) containing 1% TX-100 and 4% polyethylene glycol for 5 min (Svitkina *et al.*, 1995; Helfand *et al.*, 2002). In these experiments, 2 mM phalloidin (Invitrogen) was added to the PEM buffer to preserve actin structures. These preparations were then fixed with 2% glutaraldehyde, labeled with gold-conjugated antibodies, stained with 0.1% tannic acid/0.2% uranyl acetate, and processed by critical point drying/rotary shadowing as previously described (Svitkina *et al.*, 1995; Helfand *et al.*, 2002). Controls for these preparations involved all of the various steps and incubations described using either no antibodies or secondary gold-coupled antibodies alone. These preparations were observed with a JEOL JEM-1200EX transmission electron microscope.

ACKNOWLEDGMENTS

We thank Michael Davidson (Florida State University, Tallahassee) for the Emerald-vimentin construct and Karen Ridge (Northwestern University, Chicago, IL) for fibroblasts isolated from the $vim^{-/-}$ mouse. Thank you also to Lynne Chang and Satya Khuon for assistance with 2B2 experiments and Anne Goldman, Kyung Hee Myung, and Yuan yuan Wang for technical assistance. This study was supported by the National Institutes of Health (grant GM-036806 to R.D.G., NS-071216 to Y.I.W., and GM-057464 to K.M.G.) and the American Urological Association Foundation Research Scholar Program (B.T.H.).

REFERENCES

Abercrombie M (1961). The bases of the locomotory behaviour of fibroblasts. Exp Cell Res 8, Suppl 1188–198.

Acloque H, Adams MS, Fishwick K, Bronner-Fraser M, Nieto MA (2009). Epithelial-mesenchymal transitions: the importance of changing cell state in development and disease. J Clin Invest 119, 1438–1449.

Ando S, Tanabe K, Gonda Y, Sato C, Inagaki M (1989). Domain- and sequence-specific phosphorylation of vimentin induces disassembly of the filament structure. Biochemistry 28, 2974–2979.

Barberis L *et al.* (2009). Leukocyte transmigration is modulated by chemokine-mediated PI3Kγ-dependent phosphorylation of vimentin. Eur J Immunol 39, 1136–1146.

Bhattacharya R, Gonzalez AM, Debiase PJ, Trejo HE, Goldman RD, Flitney FW, Jones JC (2009). Recruitment of vimentin to the cell surface by β3 integrin and plectin mediates adhesion strength. J Cell Sci 122, 1390–1400.

Chan Y, Anton-Lamprecht I, Yu QC, Jackel A, Zabel B, Ernst JP, Fuchs E (1994). A human keratin 14 "knockout": the absence of K14 leads to severe epidermolysis bullosa simplex and a function for an intermediate filament protein. Genes Dev 8, 2574–2587.

Chang L, Barlan K, Chou YH, Grin B, Lakonishok M, Serpinskaya AS, Shumaker DK, Herrmann H, Gelfand VI, Goldman RD (2009). The dynamic properties of intermediate filaments during organelle transport. J Cell Sci 122, 2914–2923.

Chang L, Shav-Tal Y, Trcek T, Singer RH, Goldman RD (2006). Assembling an intermediate filament network by dynamic cotranslation. J Cell Biol 172, 747–758.

Chou YH, Bischoff JR, Beach D, Goldman RD (1990). Intermediate filament reorganization during mitosis is mediated by p34cdc2 phosphorylation of vimentin. Cell 62, 1063–1071.

Chou YH, Ngai KL, Goldman R (1991). The regulation of intermediate filament reorganization in mitosisp34cdc2 phosphorylates vimentin at a unique N-terminal site. J Biol Chem 266, 7325–7328.

Chou YH, Opal P, Quinlan RA, Goldman RD (1996). The relative roles of specific N- and C-terminal phosphorylation sites in the disassembly of intermediate filament in mitotic BHK-21 cells. J Cell Sci 109, 817–826.

Colucci-Guyon E, Portier MM, Dunia I, Paulin D, Pournin S, Babinet C (1994). Mice lacking vimentin develop and reproduce without an obvious phenotype. Cell 79, 679–694.

Consortium TU (2010). The Universal Protein Resource (UniProt) in 2010. Nucleic Acids Res 38, D142–148.

Eckes B, Colucci-Guyon E, Smola H, Nodder S, Babinet C, Krieg T, Martin P (2000). Impaired wound healing in embryonic and adult mice lacking vimentin. J Cell Sci 113, 2455–2462.

Eckes B *et al.* (1998). Impaired mechanical stability, migration and contractile capacity in vimentin-deficient fibroblasts. J Cell Sci 111, 1897–1907.

Eriksson JE, He T, Trejo-Skalli AV, Harmala-Brasken AS, Hellman J, Chou YH, Goldman RD (2004). Specific in vivo phosphorylation sites determine the assembly dynamics of vimentin intermediate filaments. J Cell Sci 117, 919–932.

Fukata M, Nakagawa M, Kaibuchi K (2003). Roles of Rho-family GTPases in cell polarisation and directional migration. Curr Opin Cell Biol 15, 590–597.

Gilles C, Polette M, Zahm JM, Tournier JM, Volders L, Foidart JM, Birembaut P (1999). Vimentin contributes to human mammary epithelial cell migration. J Cell Sci 112, 4615–4625.

Goldman AE, Moir RD, Montag-Lowy M, Stewart M, Goldman RD (1992). Pathway of incorporation of microinjected lamin A into the nuclear envelope. J Cell Biol 119, 725–735.

Goldman RD, Khuon S, Chou YH, Opal P, Steinert PM (1996). The function of intermediate filaments in cell shape and cytoskeletal integrity. J Cell Biol 134, 971–983.

Goto H, Tanabe K, Manser E, Lim L, Yasui Y, Inagaki M (2002). Phosphorylation and reorganization of vimentin by p21-activated kinase (PAK). Genes Cells 7, 91–97.

Hall A (2005). Rho GTPases and the control of cell behaviour. Biochem Soc Trans 33, 891–895.

Helfand BT, Mendez MG, Pugh J, Delsert C, Goldman RD (2003). A role for intermediate filaments in determining and maintaining the shape of nerve cells. Mol Biol Cell 14, 5069–5081.

Helfand BT, Mikami A, Vallee RB, Goldman RD (2002). A requirement for cytoplasmic dynein and dynactin in intermediate filament network assembly and organization. J Cell Biol 157, 795–806.

Helmke BP, Goldman RD, Davies PF (2000). Rapid displacement of vimentin intermediate filaments in living endothelial cells exposed to flow. Circ Res 86, 745–752.

Hendrix MJ, Seftor EA, Seftor RE, Trevor KT (1997). Experimental coexpression of vimentin and keratin intermediate filaments in human breast cancer cells results in phenotypic interconversion and increased invasive behavior. Am J Pathol 150, 483–495.

Herrmann H, Aebi U (2000). Intermediate filaments and their associates: multi-talented structural elements specifying cytoarchitecture and cytodynamics. Curr Opin Cell Biol 12, 79–90.

Herrmann H, Eckelt A, Brettel M, Grund C, Franke WW (1993). Temperature-sensitive intermediate filament assembly. Alternative structures of *Xenopus laevis* vimentin in vitro and in vivo. J Mol Biol 234, 99–113.

Herrmann H, Haner M, Brettel M, Muller SA, Goldie KN, Fedtke B, Lustig A, Franke WW, Aebi U (1996). Structure and assembly properties of the intermediate filament protein vimentin: the role of its head, rod and tail domains. J Mol Biol 264, 933–953.

Ho CL, Martys JL, Mikhailov A, Gundersen GG, Liem RK (1998). Novel features of intermediate filament dynamics revealed by green fluorescent protein chimeras. J Cell Sci 111, 1767–1778.

Hollenbeck PJ, Bershadsky AD, Pletjushkina OY, Tint IS, Vasiliev JM (1989). Intermediate filament collapse is an ATP-dependent and actin-dependent process. J Cell Sci 92, 621–631.

Howe AK (2004). Regulation of actin-based cell migration by cAMP/PKA. Biochim Biophys Acta 1692, 159–174.

Hyder CL, Pallari HM, Kochin V, Eriksson JE (2008). Providing cellular signposts–posttranslational modifications of intermediate filaments. FEBS Lett 582, 2140–2148.

Inagaki M, Nishi Y, Nishizawa K, Matsuyama M, Sato C (1987). Site-specific phosphorylation induces disassembly of vimentin filaments in vitro. Nature 328, 649–652.

Izawa I, Inagaki M (2006). Regulatory mechanisms and functions of intermediate filaments: a study using site- and phosphorylation state-specific antibodies. Cancer Sci 97, 167–174.

Janmey PA, Euteneuer U, Traub P, Schliwa M (1991). Viscoelastic properties of vimentin compared with other filamentous biopolymer networks. J Cell Biol 113, 155–160.

Janosch P *et al.* (2000). The Raf-1 kinase associates with vimentin kinases and regulates the structure of vimentin filaments. FASEB J 14, 2008–2021.

Kim H, Nakamura F, Lee W, Hong C, Perez-Sala D, McCulloch CA (2010). Regulation of cell adhesion to collagen via β1 integrins is dependent on interactions of filamin A with vimentin and protein kinase C epsilon. Exp Cell Res 316, 1829–1844.
Kirmse R, Portet S, Mucke N, Aebi U, Herrmann H, Langowski J (2007). A quantitative kinetic model for the in vitro assembly of intermediate filaments from tetrameric vimentin. J Biol Chem 282, 18563–18572.
Kosako H, Amano M, Yanagida M, Tanabe K, Nishi Y, Kaibuchi K, Inagaki M (1997). Phosphorylation of glial fibrillary acidic protein at the same sites by cleavage furrow kinase and Rho-associated kinase. J Biol Chem 272, 10333–10336.
Kosako H, Goto H, Yanagida M, Matsuzawa K, Fujita M, Tomono Y, Okigaki T, Odai H, Kaibuchi K, Inagaki M (1999). Specific accumulation of Rho-associated kinase at the cleavage furrow during cytokinesis: cleavage furrow-specific phosphorylation of intermediate filaments. Oncogene 18, 2783–2788.
Kreplak L, Bar H, Leterrier JF, Herrmann H, Aebi U (2005). Exploring the mechanical behavior of single intermediate filaments. J Mol Biol 354, 569–577.
Kreplak L, Herrmann H, Aebi U (2008). Tensile properties of single desmin intermediate filaments. Biophys J 94, 2790–2799.
Kural C, Serpinskaya AS, Chou YH, Goldman RD, Gelfand VI, Selvin PR (2007). Tracking melanosomes inside a cell to study molecular motors and their interaction. Proc Natl Acad Sci USA 104, 5378–5382.
Lamb NJ, Fernandez A, Feramisco JR, Welch WJ (1989). Modulation of vimentin containing intermediate filament distribution and phosphorylation in living fibroblasts by the cAMP-dependent protein kinase. J Cell Biol 108, 2409–2422.
Lawrence JB, Singer RH (1986). Intracellular localization of messenger RNAs for cytoskeletal proteins. Cell 45, 407–415.
Li J, Ning Y, Hedley W, Saunders B, Chen Y, Tindill N, Hannay T, Subramaniam S (2002). The Molecule Pages database. Nature 420, 716–717.
Lin YC, Broedersz CP, Rowat AC, Wedig T, Herrmann H, Mackintosh FC, Weitz DA (2010). Divalent cations crosslink vimentin intermediate filament tail domains to regulate network mechanics. J Mol Biol 399, 637–644.
Matsudaira P (1994). Actin crosslinking proteins at the leading edge. Semin Cell Biol 5, 165–174.
Meier M, Padilla GP, Herrmann H, Wedig T, Hergt M, Patel TR, Stetefeld J, Aebi U, Burkhard P (2009). Vimentin coil 1A-A molecular switch involved in the initiation of filament elongation. J Mol Biol 390, 245–261.
Mendez MG, Kojima S-I, Goldman RD (2010). Vimentin induces changes in cell shape, motility, and adhesion during the epithelial to mesenchymal transition. FASEB J 24, 1838–1851.
Mogilner A, Keren K (2009). The shape of motile cells. Curr Biol 19, R762–771.
Moir RD, Donaldson AD, Stewart M (1991). Expression in *Escherichia coli* of human lamins A and C: influence of head and tail domains on assembly properties and paracrystal formation. J Cell Sci 99, 363–372.
Perlson E, Hanz S, Ben-Yaakov K, Segal-Ruder Y, Seger R, Fainzilber M (2005). Vimentin-dependent spatial translocation of an activated MAP kinase in injured nerve. Neuron 45, 715–726.
Prahlad V, Yoon M, Moir RD, Vale RD, Goldman RD (1998). Rapid movements of vimentin on microtubule tracks: kinesin-dependent assembly of intermediate filament networks. J Cell Biol 143, 159–170.
Schoumacher M, Goldman RD, Louvard D, Vignjevic DM (2010). Actin, microtubules, and vimentin intermediate filaments cooperate for elongation of invadopodia. J Cell Biol 189, 541–556.
Sihag RK, Inagaki M, Yamaguchi T, Shea TB, Pant HC (2007). Role of phosphorylation on the structural dynamics and function of types III and IV intermediate filaments. Exp Cell Res 313, 2098–2109.
Sin W-C, Chen X-Q, Leung T, Lim L (1998). RhoA-binding kinase α translocation is facilitated by the collapse of the vimentin intermediate filament network. Mol Cell Biol 18, 6325–6339.
Sivaramakrishnan S, DeGiulio JV, Lorand L, Goldman RD, Ridge KM (2008). Micromechanical properties of keratin intermediate filament networks. Proc Natl Acad Sci USA 105, 889–894.
Small JV, Resch GP (2005). The comings and goings of actin: coupling protrusion and retraction in cell motility. Curr Opin Cell Biol 17, 517–523.
Small JV, Stradal T, Vignal E, Rottner K (2002). The lamellipodium: where motility begins. Trends Cell Biol 12, 112–120.
Strelkov SV, Herrmann H, Geisler N, Wedig T, Zimbelmann R, Aebi U, Burkhard P (2002). Conserved segments 1A and 2B of the intermediate filament dimer: their atomic structures and role in filament assembly. EMBO J 21, 1255–1266.
Svitkina TM, Verkhovsky AB, Borisy GG (1995). Improved procedures for electron microscopic visualization of the cytoskeleton of cultured cells. J Struct Biol 115, 290–303.
Takenawa T, Suetsugu S (2007). The WASP-WAVE protein network: connecting the membrane to the cytoskeleton. Nat Rev Mol Cell Biol 8, 37–48.
Vora HH, Patel NA, Rajvik KN, Mehta SV, Brahmbhatt BV, Shah MJ, Shukla SN, Shah PM (2009). Cytokeratin and vimentin expression in breast cancer. Int J Biol Markers 24, 38–46.
Weinstein DE, Shelanski ML, Liem RK (1991). Suppression by antisense mRNA demonstrates a requirement for the glial fibrillary acidic protein in the formation of stable astrocytic processes in response to neurons. J Cell Biol 112, 1205–1213.
Windoffer R, Kolsch A, Woll S, Leube RE (2006). Focal adhesions are hotspots for keratin filament precursor formation. J Cell Biol 173, 341–348.
Wu YI, Frey D, Lungu OI, Jaehrig A, Schlichting I, Kuhlman B, Hahn KM (2009). A genetically encoded photoactivatable Rac controls the motility of living cells. Nature 461, 104–108.
Yamada H, Abe T, Li SA, Masuoka Y, Isoda M, Watanabe M, Nasu Y, Kumon H, Asai A, Takei K (2009). Dynasore, a dynamin inhibitor, suppresses lamellipodia formation and cancer cell invasion by destabilizing actin filaments. Biochem Biophys Res Commun 390, 1142–1148.
Yoon KH, Yoon M, Moir RD, Khuon S, Flitney FW, Goldman RD (2001). Insights into the dynamic properties of keratin intermediate filaments in living epithelial cells. J Cell Biol 153, 503–516.
Yoon M, Moir RD, Prahlad V, Goldman RD (1998). Motile properties of vimentin intermediate filament networks in living cells. J Cell Biol 143, 147–157.
Zhang Q *et al*. (2009). Nuclear factor-κB-mediated transforming growth factor-β-induced expression of vimentin is an independent predictor of biochemical recurrence after radical prostatectomy. Clin Cancer Res 15, 3557–3567.
Zhu QS *et al*. (2011). Vimentin is a novel AKT1 target mediating motility and invasion. Oncogene 30, 457–470.